

Copy No.

SID 67-212-1

A STUDY OF LONGITUDINAL OSCILLATIONS OF PROPELLANT
TANKS AND WAVE PROPAGATIONS IN FEED LINES

PART I - PROPAGATING PRESSURE WAVES IN A FLUID-
FILLED CYLINDRICAL SHELL

31 May 1967

NAS8-11490



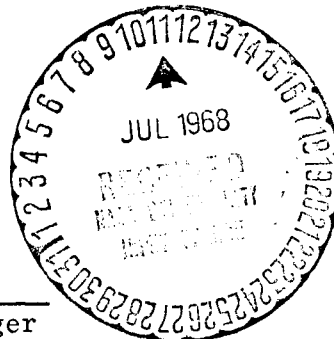
Prepared by

John S. Kanno, Staff Investigator
Clement L. Tai, Principal Investigator

Approved by

F. C. Hung
F. C. Hung, Program Manager
Structures and Materials

L. A. Harris
L. A. Harris, Assistant Manager
Science and Technology



NORTH AMERICAN AVIATION, INC.
SPACE and INFORMATION SYSTEMS DIVISION

GPO PRICE \$ _____

CFSTI PRICE(S) \$ _____

Hard copy (HC) 3.00

Microfiche (MF) _____

N 68-30087

(ACCESSION NUMBER)

(THRU)

76
(PAGES)

(CODE)

CR-61884
(NASA CR OR TMX OR AD NUMBER)

12
(CATEGORY)

FACILITY FORM 602

Copy No.

SID 67-212-1

A STUDY OF LONGITUDINAL OSCILLATIONS OF PROPELLANT
TANKS AND WAVE PROPAGATIONS IN FEED LINES
PART I - PROPAGATING PRESSURE WAVES IN A FLUID-
FILLED CYLINDRICAL SHELL

31 May 1967

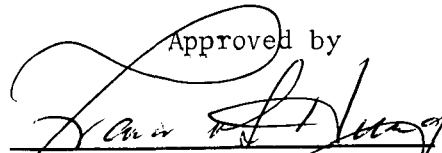
NAS8-11490

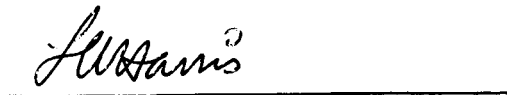


Prepared by

John S. Kanno, Staff Investigator
Clement L. Tai, Principal Investigator

Approved by


F. C. Hung, Program Manager
Structures and Materials


L. A. Harris, Assistant Manager
Science and Technology

NORTH AMERICAN AVIATION, INC.
SPACE and INFORMATION SYSTEMS DIVISION



PRECEDING PAGE BLANK NOT FILMED.

FOREWORD

This report was prepared by the Space and Information Systems Division of North American Aviation, Inc., Downey, California, for the George C. Marshall Space Flight Center, National Aeronautics and Space Administration, Huntsville, Alabama, under the Supplemental Agreement Modification No. 2 of Contract NAS8-11490, "*Study of Longitudinal Oscillations of Propellant Tanks and Wave Propagations in Feed Lines,*" dated April 6, 1966. Dr. George F. McDonough (Principal) and Mr. Robert S. Ryan (Alternate) of Aero-Astrodynamic Laboratory, MSFC, are Contracting Officer Representatives. The work is published in two separate parts:

PART I - Propagating Pressure Waves in a Fluid Filled Cylindrical Shell

PART II - Longitudinal Oscillation of a Liquid-Filled Elastic Cylindrical Tank with a Flexible Inverted Conical Bulkhead

The project was carried out by the Vehicle Dynamics Branch, Structures and Materials Department of Research, Engineering and Testing Division, S&ID. Dr. F. C. Hung was the Program Manager for North American Aviation, Inc. The study was conducted by Dr. Clement L. Tai (Principal Investigator), Dr. Shoichi Uchiyama and Mr. John S. Kanno.

The computer program was developed by Mr. Miyashiro.



PRECEDING PAGE BLANK NOT FILMED.

ABSTRACT

The properties of the propagating pressure waves in a fluid-filled cylindrical shell as established by a two-dimensional theory of the fluid are derived. The fluid is treated as an axially symmetric, inviscid, and compressible liquid. The cylinder bounding the fluid is treated in accordance with shell theory. The bending rigidity of the shell wall is included; however, the transverse shearing rigidity is ignored.

The equations of motion of the fluid and shell perturbations with respect to a steady-state flow are reviewed. For propagating harmonic hydroelastic waves, it is shown that the nature of the fluid pressures depends on whether or not the phase velocity of the wave exceeds the acoustic velocity. A simplification of the solution of the equations of motion is resolved for steady-state flows having flow velocities less than the phase velocities of the propagating waves.

The calculated properties of the propagating pressure waves typical of the propellant feed lines of rocket propellant systems are also presented. Finally, the perspective of the pertinent behavioral attributes showing in what order of occurrence of the water hammer behavior, the shell wall vibrations as influenced by the fluid, and the acoustic behavior of the fluid is reviewed.



PRECEDING PAGE BLANK NOT FILMED.

CONTENTS

| <u>Title</u> | <u>Page</u> |
|--|-------------|
| FOREWORD | iii |
| ABSTRACT | v |
| SYMBOLS | xi |
| INTRODUCTION | 1 |
| REVIEW OF THE EQUATIONS OF MOTION | 5 |
| SOLUTION FOR PROPAGATING HARMONIC WAVES | 11 |
| EXAMINATION OF THE CHARACTERISTIC EQUATION | 19 |
| The Properties of the Propagating Waves Having Subsonic Phase Velocities, $\lambda^2 \leq \kappa^2$ | 22 |
| The Properties of the Propagating Waves Having Supersonic Phase Velocities, $\lambda^2 \geq \kappa^2$ | 29 |
| CALCULATED RESPONSE PROPERTIES TYPICAL OF THE FEED LINES OF ROCKET PROPELLANT SYSTEMS | 35 |
| CONCLUDING REMARKS AND RECOMMENDATIONS | 39 |
| REFERENCES | 43 |



PRECEDING PAGE BLANK NOT FILMED.

ILLUSTRATIONS

| <u>Table</u> | | <u>Page</u> |
|-------------------|--|-------------|
| 1 | Typical Propellant/Duct Parameters | 45 |
| <u>Figure</u> | | |
| 1 | Coordinates, Fluid Velocity Components & Shell Dis- placement Components | 47 |
| 2 | Typical Shell Wall Loads for Subsonic & Supersonic Phase Velocities | 48 |
| 3 | The Simultaneous Solution $\psi_1(\eta^2) = Y(\eta^2)$ | 49 |
| 4 | $(\psi_2/\zeta^2\sigma) - \zeta^2$ | 50 |
| 5 | $G(\kappa^2/\zeta^2) - (\kappa^2/\zeta^2)$ | 51 |
| 6 | Mapping the Solution of $(\psi_2/\zeta^2\sigma) = G$ | 52 |
| 7 | Supersonic Branches of the Frequency-Wavelength Relationship | 53 |
| 8 | The Lower Branch Frequency-Wavelength Relationship | 54 |
| 9 | The Lower Branch Phase Velocity vs Wave Number Relationship | 55 |
| 10a,b | $(\psi_2/\zeta^2\sigma) - \zeta^2$ for $\mu = 40.9$ and $\sigma = 0.0571$ | 56 |
| 11a,b,c | $G - (\kappa^2/\zeta^2)$ for $\sigma = 0.0571$ and $v^2 = 0.1089$ | 58 |
| 12a,b | $(\psi_2/\zeta^2\sigma) - \zeta^2$ for $\mu = 2.54$ and $\sigma = 0.920$ | 61 |
| 13 | $G - (\kappa^2/\zeta^2)$ for $\sigma = 0.920$ and $v^2 = 0.1089$ | 63 |
| 14 | Graphical solution of $(\zeta_p/\mu) = J_0(\zeta_p)/J_1(\zeta_p)$ | 64 |
| 15a,b | The Frequency vs Wavelength Relationship for $\sigma = 0.0571, \mu = 40.9$ and $c = 4420$ | 65 |
| 16a,b | The Frequency vs Wavelength Relationship for $\sigma = 0.920, \mu = 2.54$ and $c = 17730$ | 67 |



| <u>Figure</u> | | <u>Page</u> |
|---------------|--|-------------|
| 17a | Response Typical of the Hydroelastic Propagating Wave Having the Subsonic Phase Velocity | 69 |
| 17b | Response Typical of the Hydroelastic Propagating Wave Having the Supersonic First Mode Phase Velocity . . | 70 |
| 17c | Response Typical of the Hydroelastic Propagating Wave Having the Supersonic Second Mode Phase Velocity . . | 71 |



SYMBOLS

| | |
|------------|---|
| r, x | Reference coordinates of the fluid/shell combination designating the radial and longitudinal positions, respectively. |
| v_r, v_x | Radial and longitudinal components of fluid velocity, respectively. |
| V, v | Steady-state and perturbational components of the longitudinal component of fluid velocity, respectively. |
| p | Fluid pressure |
| ρ | Fluid mass density |
| ρ_0 | Steady-state fluid mass density. |
| B | Bulk modulus of the fluid. |
| c | Acoustic velocity in the fluid. |
| ϕ | Velocity potential of the fluid |
| a | Cylinder radius |
| w, u | Radial and longitudinal displacement components of the shell. |
| h | Wall thickness of the shell. |
| m | Mass per unit surface area of the shell. |
| ρ_s | Mass density of the shell material. |
| E | Young's modulus of the shell material. |
| ν | Poisson's ratio of the shell material |
| D | Extensional rigidity of the shell. |
| K | Wall bending rigidity of the shell |
| c_s | Elastic wave velocity in the shell |
| ω | Frequency |



| | |
|---|---|
| ℓ | Half-wavelength |
| \tilde{v} | Phase velocity of a propagating harmonic wave |
| k | Wave number |
| I_0, I_1 | Modified Bessel functions of the first kind, and zero and first orders, respectively. |
| J_0, J_1 | Bessel functions of the first kind, and zero and first orders, respectively. |
| $\lambda^2 \equiv \left(\frac{\omega a}{c}\right)^2$ | Frequency parameter |
| $\kappa^2 \equiv \left(\frac{\pi a}{\ell}\right)^2$ | Wave number parameter |
| $\left(\frac{v}{c}\right)^2 \equiv \left(\frac{\omega \ell}{\pi c}\right)^2$ | Phase velocity parameter |
| $\mu \equiv \frac{\rho_0 a}{m}$ | Mass ratio parameter |
| $\sigma \equiv \left(\frac{c}{c_s}\right)^2 (1-v^2)$ | Speed ratio parameter |
| $\epsilon \equiv \frac{K}{a^2 D}$ | Rigidity ratio parameter |
| $\left. \begin{aligned} \eta^2 &\equiv \kappa^2 - \lambda^2 \geq 0 \\ \zeta^2 &\equiv \lambda^2 - \kappa^2 \geq 0 \end{aligned} \right\}$ | New unknowns of the characteristic equation |
| $\psi_1(\eta)^2 \equiv \left(1 + \frac{\mu I_0(\eta)}{\eta I_1(\eta)}\right)^{-1}$ | |
| | Auxiliary function of the characteristic equation |



$\psi_2(\eta^2) \equiv \left(1 - \frac{\mu J_0(\zeta)}{\zeta J_1(\zeta)}\right)^{-1}$ Auxiliary function of the characteristic equation

$Y(\eta^2), G\left(\frac{\kappa^2}{\zeta^2}\right)$ Auxiliary functions of the characteristic function (cf., Equations 43 and 53).

Δ cf., Figure 6.



INTRODUCTION

The theory of the propagation of pressure waves in a fluid-filled cylindrical shell, exemplified by the one-dimensional theory of water hammer behavior, has numerous practical applications. The various engineering problems to which the one-dimensional theory has been successfully applied include the analysis of the transmission dynamics of fluid power control systems, Reference [1], and the study of pressure transients occurring in the pipelines of hydraulic storage and distribution systems, Reference [2]. More recently, the one-dimensional theory has been applied to explain the unsteady hydroelastic pressure surges believed to occur in the propellant feed lines of rocket propellant systems, Reference [3], and is also currently instrumental in the theoretical examination of launch vehicle longitudinal oscillations, Reference [4]. Although the one-dimensional theory has widespread practical application, it does have definite limitations. These limitations, thus far, have not been fully explored.

Briefly, the one-dimensional theory of the pressure waves in a fluid-filled cylindrical shell is based on two governing principles. First, the hydrodynamic mechanism involves only the longitudinal component of fluid momentum. Second, the hydroelastic mechanism, based on the principle only the fluid longitudinal continuity is to be maintained, involves the fluid compressibility and the change of the cross-sectional area of the elastic cylinder bounding the fluid caused by the static structural response to the fluid pressures. For a continuous train of free harmonic pressure waves, the theory describes the velocity of wave propagation as constant regardless of the wavelength. The velocity of wave propagation depending only on the sectional physical properties, is defined by the equation for thin walled cylinders,

$$\left(\frac{\tilde{v}}{c}\right)^2 = \frac{1}{1 + \frac{B}{E} \cdot \frac{2a}{h}} \quad (1)$$

Reference [2]. For harmonic standing wave vibrations, the theory describes the frequency of the response to be inversely proportional to the wavelength exhibited. That is,

$$\omega = \frac{\pi}{\lambda} \cdot \frac{c}{\sqrt{1 + \frac{B}{E} \cdot \frac{2a}{h}}} \quad (2)$$



Intrinsic to the one-dimensional theory is the underlying assumption that the longitudinal rate of change of the shell wall deformation is directly proportional to the longitudinal rate of change of the acting pressure distribution. In the extreme case, for discontinuous longitudinal pressure distributions, it is implied that longitudinal discontinuities of the shell wall deformation occur. But this is not physically possible. Furthermore, for sudden longitudinal changes of the structural deformation, not only is the deformation continuous but the shell wall bending resistance is just as significant as the membrane resistance already included in the theory. Finally, due to the basic suppositions that the flow field is one-dimensional and that the shell response is static, the basic water hammer theory does not reveal the nature of occurrence of either the propagating acoustic waves of the fluid or the propagating shell wall vibrations.

The purpose of the theoretical analysis presented in this report is to examine the two-dimensional, axially symmetric, mathematical extension of the basic theory and to establish the perspective of the pertinent dynamic properties showing in what order the water hammer behavior of the one-dimensional theory, the acoustic behavior of the fluid, and the shell wall vibrations occur. Work of this type is not new. Several papers pertinent to the study of propagating waves in either a cylindrical shell or the combination of the cylindrical shell and a compressible inviscid fluid are readily available.

For example, prompted by the problem of the radiation of underwater noise, the axially symmetric free vibrations of an infinitely long fluid-filled cylindrical shell immersed in an infinite fluid has been studied by Junger, Reference [5], and the forced and free vibrations of an infinitely long cylindrical shell immersed in an infinite acoustic medium has been studied by Bleich and Baron, Reference [6]. The primary concern, in both papers, is for the hydroelastic mechanism generating the acoustic pressures and the nature of the radiation of the pressures throughout the surrounding fluid. More recently, the behavior of an internal compressible fluid column interacting with a thin pressurized cylindrical shell has been studied by Berry and Reissner, Reference [7]. In this work, the breathing modes of shell behavior and not the axially symmetric mode of shell behavior are examined. Although the analytical principles and procedures of these papers apply directly to the work presented in this report, the results published in these papers do not.

Other work more directly related to the study presented here includes the analyses by Herrman and Mirsky of the propagating harmonic vibrations of a cylindrical tube, References [8] and [9]. Prompted by the problem of relating the theory of elasticity and the theory of shells, Herrman and Mirsky reviewed the axially symmetric behavior of thick-walled cylindrical shells. Their examination of the low frequency vibration mode reveals that two distinct regimes of shell wall behavior exist, separated by the so-



called transition wavelength

$$\left(\frac{\ell_t}{\pi a}\right)^2 \cong 0.297 \left(\frac{h}{a}\right) \quad (3)$$

Their work shows that, for wavelengths longer than the transition wavelength, the shell wall response described by the sophisticated theory is essentially identical to the response described by the elementary shell theory which reflects only the shell mass and the membrane rigidity. For wavelengths shorter than the transition wavelength, the shell wall response described by the sophisticated theory is essentially the response described by the theory of flat plates and, consequently, reflects either or both the shell wall bending rigidity and the transverse shearing rigidity depending on the wall thickness of the shell. These conclusions resolved by Herrman and Mirsky are pertinent to the study presented in this report.



PRECEDING PAGE BLANK NOT FILMED.

REVIEW OF THE EQUATIONS OF MOTION

The hydroelastic behavior of a cylindrical shell filled with a flowing fluid is governed by two essentially independent sets of partial differential equations. The first set pertains to the axially symmetric dynamic behavior of the cylindrical shell wall. The physical constraints - the compatibility between the fluid and the shell radial velocity components at the shell wall and the shell wall compliance to the fluid pressures generated at the wall - interconnect the fluid and the shell equations of motion. These equations of motion are otherwise unrelated.

The assigned cylindrical coordinates, the axially symmetric fluid velocity components and the shell wall displacement components pertinent to the equations of motion are depicted in Figure 1. The steady-state fluid velocity is denoted by V . The unsteady fluid and shell wall perturbations are denoted by $v_r(r,x,t)$, $v_x(r,x,t)$ and $w(x,t)$, $u(x,t)$, respectively. The outward acting distributed fluid pressure load on the shell wall, not shown in Figure 1, is assigned the positive sense.

The equations of motion of the fluid pertinent to this study are formulated using the fundamental principles presented in References [10] and [11]. The behavior of the compressible inviscid liquid in the absence of fluid body forces is governed by the law of fluid continuity,

$$\frac{1}{\rho} \left(\frac{\partial \rho}{\partial t} + v_r \frac{\partial \rho}{\partial r} + v_x \frac{\partial \rho}{\partial x} \right) + \frac{\partial v_r}{\partial r} + \frac{v_r}{r} + \frac{\partial v_x}{\partial x} = 0 \quad (4)$$

the Eulerian equations of motion,

$$\begin{aligned} \frac{\partial v_r}{\partial t} + v_r \frac{\partial v_r}{\partial r} + v_x \frac{\partial v_r}{\partial x} &= - \frac{1}{\rho} \frac{\partial p}{\partial r} \\ \frac{\partial v_x}{\partial t} + v_r \frac{\partial v_x}{\partial r} + v_x \frac{\partial v_x}{\partial x} &= - \frac{1}{\rho} \frac{\partial p}{\partial x} \end{aligned} \quad (5)$$

and the liquid acoustical pressure-density relationship,

$$c^2 = \frac{\partial p}{\partial \rho} = \frac{B}{\rho_0} \quad (6)$$



The acoustic velocity, c , defined by Equation (6) is essentially constant for a wide variation of pressure, so long as the minimum pressure exceeds the vapor pressure of the liquid, and depends on the bulk modulus of elasticity, B , as shown. These equations involving unknown velocity components, density and pressure may be replaced by a single relationship involving an unknown scalar variable.

The persistence of irrotationality of an inviscid fluid permits

$$\frac{\partial v_r}{\partial x} = \frac{\partial v_x}{\partial r} = \frac{\partial v}{\partial r}$$

and the velocity potential, $\phi(r,x,t)$, occurring consistent with the relationships

$$\frac{\partial \phi}{\partial r} = v_r \quad \text{and} \quad \frac{\partial \phi}{\partial x} = v_x - V = v \quad (7)$$

to be introduced. It follows that Equation (5) can be integrated with respect to space - that is, not necessarily along a streamline - to yield the Bernoulli equation

$$\frac{\partial \phi}{\partial t} + \frac{1}{2}(v_r^2 + v_x^2) + \int \frac{dp}{\rho} = F(t)$$

As indicated in Reference [11], the constant of integration, $F(t)$, can be superimposed on $\frac{\partial \phi}{\partial t}$ without altering the properties of the flow. Consequently, it is permitted to replace the preceding equation with

$$\frac{\partial \phi}{\partial t} + \frac{1}{2}(v_r^2 + v_x^2) + \int \frac{dp}{\rho} = C \quad (8)$$

where C is a constant evaluated anywhere in the flow. The partial differentiation of Equation (8) with respect to time yields

$$\frac{\partial^2 \phi}{\partial t^2} + \frac{1}{2} \frac{\partial}{\partial t} (v_r^2 + v_x^2) + \frac{1}{\rho} \frac{\partial p}{\partial t} = 0$$



or

$$\frac{1}{\rho} \frac{\partial p}{\partial t} = - \frac{\partial^2 \phi}{\partial t^2} - \frac{1}{2} \frac{\partial}{\partial t} (v_r^2 + v_x^2). \tag{9}$$

It follows from Equation (6) that

$$\frac{\partial p}{\partial t} = c^2 \frac{\partial \rho}{\partial t}, \quad \frac{\partial p}{\partial r} = c^2 \frac{\partial \rho}{\partial r} \quad \text{and} \quad \frac{\partial p}{\partial x} = c^2 \frac{\partial \rho}{\partial x} \tag{10}$$

Consequently, Equations (9) and (5) using Equation (10) yield

$$\frac{1}{\rho} \frac{\partial \rho}{\partial t} = - \frac{1}{c^2} \left\{ \frac{\partial^2 \phi}{\partial t^2} + \frac{1}{2} \frac{\partial}{\partial t} (v_r^2 + v_x^2) \right\}$$

$$\frac{1}{\rho} \frac{\partial \rho}{\partial r} = - \frac{1}{c^2} \left\{ \frac{\partial v_r}{\partial t} + v_r \frac{\partial v_r}{\partial r} + v_x \frac{\partial v_r}{\partial x} \right\}$$

$$\frac{1}{\rho} \frac{\partial \rho}{\partial x} = - \frac{1}{c^2} \left\{ \frac{\partial v_x}{\partial t} + v_r \frac{\partial v_x}{\partial r} + v_x \frac{\partial v_x}{\partial x} \right\}$$

Moreover, using these equations, it is easily shown that Equation (4) is identical to

$$\begin{aligned} - \frac{1}{c^2} \left\{ \frac{\partial^2 \phi}{\partial t^2} + \frac{\partial}{\partial t} (v_r^2 + v_x^2) + v_r^2 \frac{\partial v_r}{\partial r} + v_r v_x \left(\frac{\partial v_r}{\partial x} + \frac{\partial v_x}{\partial r} \right) + v_x^2 \frac{\partial v_x}{\partial x} \right\} \\ + \frac{\partial v_r}{\partial r} + \frac{v_r}{r} + \frac{\partial v_x}{\partial x} = 0 \end{aligned} \tag{11}$$

where

$$v_r = \frac{\partial \phi}{\partial r} \quad \text{and} \quad v_x = V + v, \quad v = \frac{\partial \phi}{\partial x}$$



Equation (11) is a nonlinear partial differential equation involving the unknown, $\phi(r,x,t)$. If v_r and v are both sufficiently small, the higher order products of v_r , v and their partial derivatives appearing in Equations (8) and (11) can be ignored. What remains - that is,

$$\frac{\partial \phi}{\partial t} + \frac{1}{2}(V^2 + 2V \cdot v) + \int \frac{dp}{\rho} = C \quad (12)$$

and

$$-\frac{1}{c^2} \left\{ \frac{\partial^2 \phi}{\partial t^2} + 2V \frac{\partial v}{\partial t} + V^2 \frac{\partial v}{\partial x} \right\} + \frac{\partial v_r}{\partial r} + \frac{v_r}{r} + \frac{\partial v}{\partial x} = 0$$

or

$$-\frac{1}{c^2} \left\{ \frac{\partial^2 \phi}{\partial t^2} + 2V \frac{\partial^2 \phi}{\partial t \partial x} \right\} + \frac{\partial^2 \phi}{\partial r^2} + \frac{1}{r} \frac{\partial \phi}{\partial r} + \left(1 - \frac{V^2}{c^2} \right) \frac{\partial^2 \phi}{\partial x^2} = 0 \quad (13)$$

respectively, describes the linear behavior of the fluid perturbations. For small fluid perturbations, it also follows that

$$\int \frac{dp}{\rho} \cong \frac{p_0}{\rho_0} + \frac{p}{\rho_0}$$

where p denotes the pressure perturbation. It is convenient to assign

$C = \frac{1}{2}V^2 + \frac{p_0}{\rho_0}$ and replace Equation (12) with

$$\frac{\partial \phi}{\partial t} + V \cdot v + \frac{p}{\rho_0} = 0$$

or

$$p = -\rho_0 \left(\frac{\partial \phi}{\partial t} + V \cdot \frac{\partial \phi}{\partial x} \right) \quad (14)$$



To complete the formulation of the linearized fluid behavior, the radial component of the fluid velocity for a fluid particle located at the wall of the cylinder is noted to be

$$v_r(a, x, t) \cong \frac{\partial \delta}{\partial t} + V \cdot \frac{\partial \delta}{\partial x}$$

where $\delta(x, t)$ denotes the radial displacement of the fluid particle located at $r = a$. However, since the fluid at the wall of the cylinder is physically constrained to move with the cylinder,

$$\delta(x, t) = w(x, t)$$

and the preceding relationship is replaced by the boundary condition

$$v_r(a, x, t) \cong \frac{\partial w}{\partial t} + V \frac{\partial w}{\partial x} \quad (15)$$

The axially symmetric equations of motion of the shell based, for example, on the simplified elastic laws of Reference [12] are

$$D \left(\frac{\partial^2 u}{\partial x^2} + \frac{\nu}{a} \frac{\partial w}{\partial x} \right) - m \frac{\partial^2 u}{\partial t^2} = 0$$

$$K \frac{\partial^4 w}{\partial x^4} + \left(D \frac{w}{a^2} + \frac{\nu}{a} \frac{\partial u}{\partial z} \right) + m \frac{\partial^2 w}{\partial t^2} = p(a, x, t) \quad (16)$$

where according to Flügge's nomenclature

$$D \equiv \frac{Eh}{1-\nu^2} \quad \text{and} \quad K \equiv \frac{Eh^3}{12(1-\nu^2)}$$

These equations include the shell wall bending rigidity in addition to the membrane rigidity. As shown in Reference [8] and indicated by Equation (3) the shell wall bending rigidity for harmonic vibrations of the shell is not significant unless the wavelength of the vibration is quite short.



To summarize the preceding survey of the basic relationships pertinent to this study, Equations (13) and (16) describe the individual fluid and shell behaviors, respectively. The behaviors of the fluid and the shell are interconnected by the fluid pressure generated at the fluid/shell interface, Equation (14), and the compatibility of the fluid and shell radial velocity components at the fluid/shell interface, Equation (15).



SOLUTION FOR PROPAGATING HARMONIC WAVES

The properties of the propagating free harmonic hydroelastic waves are established by considering the velocity potential of the fluid to be

$$\phi(r, x, t) = A \Phi_1(r) e^{i\left(\frac{\pi}{\ell_1} x - \omega t\right)} + B \Phi_2(r) e^{i\left(\frac{\pi}{\ell_2} x + \omega t\right)} \quad (17)$$

where A and B denote the arbitrary constants which are used to assign the intensities of the harmonic wave trains propagating to the right in the direction of V and propagating to the left opposite to the direction of V, respectively. The frequency of the two wave trains is denoted by ω and the half-wavelengths of the downstream directed and upstream directed waves are denoted by ℓ_1 and ℓ_2 , respectively. The functions $\Phi_1(r)$ and $\Phi_2(r)$, are determined by the basic equations of the fluid. Equation (17) written in terms of the phase velocities of the two waves is

$$\phi(r, x, t) = A \Phi_1(r) e^{ik_1(x - \tilde{v}_1 t)} + B \Phi_2(r) e^{ik_2(x + \tilde{v}_2 t)} \quad (18)$$

where the phase velocities and wave numbers are denoted by

$$\tilde{v}_1 = \frac{\omega \ell_1}{\pi}, \quad \tilde{v}_2 = \frac{\omega \ell_2}{\pi}$$

and

$$k_1 = \frac{\pi}{\ell_1}, \quad k_2 = \frac{\pi}{\ell_2}$$

respectively. Only real phase velocities and wave numbers consistent with propagating waves are considered in this development. Nonpropagating properties of the behavior are believed to be nonessential to the problem examined and, consequently, are ignored.

The corresponding characteristic properties of the fluid, obtained by substituting the pertinent partial derivatives of Equation (17) into Equation (13), are established by



$$\left[\Phi_1'' + \frac{1}{r} \Phi_1' + \left\{ \left(\frac{\omega}{c} \right)^2 \left(1 - \frac{V\pi}{\omega \ell_2} \right)^2 - \left(\frac{\pi}{\ell_1} \right)^2 \right\} \Phi_1 \right] A e^{i \left(\frac{\pi}{\ell_1} x - \omega t \right)}$$

$$+ \left[\Phi_2'' + \frac{1}{r} \Phi_2' + \left\{ \left(\frac{\omega}{c} \right)^2 \left(1 + \frac{V\pi}{\omega \ell_2} \right)^2 - \left(\frac{\pi}{\ell_2} \right)^2 \right\} \Phi_2 \right] B e^{i \left(\frac{\pi}{\ell_2} x + \omega t \right)}$$

or, for $A \neq 0$ and $B \neq 0$, by the ordinary differential equations

$$\Phi_1'' + \frac{1}{r} \Phi_1' + \beta_1^2 \Phi_1 = 0 \quad (19)$$

and

$$\Phi_2'' + \frac{1}{r} \Phi_2' + \beta_2^2 \Phi_2 = 0 \quad (20)$$

where

$$\beta_1^2 \equiv \left(\frac{\omega}{c} \right)^2 \left(1 - \frac{V\pi}{\omega \ell_2} \right)^2 - \left(\frac{\pi}{\ell_1} \right)^2$$

$$\beta_2^2 \equiv \left(\frac{\omega}{c} \right)^2 \left(1 + \frac{V\pi}{\omega \ell_2} \right)^2 - \left(\frac{\pi}{\ell_2} \right)^2$$

Both Equations (19) and (20) are Bessel's differential equations of zero order. Consequently,

$$\Phi_1(r) = J_0(\beta_1 r) \quad , \quad \Phi_2(r) = J_0(\beta_2 r) \quad (21)$$

Since both $\Phi_1(r)$ and $\Phi_2(r)$ must be finite at the origin, the Bessel functions of the second kind, $Y_0(\beta_1 r)$ and $Y_0(\beta_2 r)$, are not admissible. The modified Bessel functions of zero order and of the first kind for imaginary arguments, $\beta_1 r$ and $\beta_2 r$, are also pertinent representations



of the fluid behavior. The analytical forms of β_1^2 and β_2^2 are nearly identical. The essential difference between the two reflects the ratios of the steady-state velocity to the phase velocities of the waves,

$$\frac{V\pi}{\omega\ell_1} = \frac{V}{\tilde{v}_1} \quad \text{and} \quad \frac{V\pi}{\omega\ell_2} = \frac{V}{\tilde{v}_2}$$

For most practical applications, the steady-state velocity is considerably less than the phase velocity of the propagating wave and, therefore, for

$$\ell_1 = \ell_2 \equiv \ell$$

it follows that

$$\beta_1^2 \cong \beta_2^2 \equiv \beta^2 \equiv \left(\frac{\omega}{c}\right)^2 - \left(\frac{\pi}{\ell}\right)^2$$

and

$$\Phi_1(r) \cong \Phi_2(r) \equiv \Phi(r) \equiv J_0(\beta r)$$

The corresponding pressure of the fluid, in accordance with Equation (14) is

$$\begin{aligned} p(r,x,t) &= -\rho_0 \left(\frac{\partial \phi}{\partial t} + V \frac{\partial \phi}{\partial x} \right) \\ &= \rho_0 \omega \left\{ \left(1 - \frac{V\pi}{\omega\ell_1} \right) \Phi_1(r) i A e^{i\left(\frac{\pi}{\ell_1} x - \omega t\right)} \right. \\ &\quad \left. - \left(1 + \frac{V\pi}{\omega\ell_2} \right) \Phi_2(r) i B e^{i\left(\frac{\pi}{\ell_2} x + \omega t\right)} \right\} \end{aligned} \quad (22)$$

The response of the shell wall to the applied fluid pressures, in accordance with Equation (16), will be assumed to take the following harmonic form:



$$\begin{aligned}
 w(x,t) &= \tilde{w}_1(x,t) + \tilde{w}_2(x,t) \\
 &= W_1 e^{i\left(\frac{\pi}{\ell_1} x - \omega t\right)} + W_2 e^{i\left(\frac{\pi}{\ell_2} x + \omega t\right)} \\
 u(x,t) &= \tilde{u}_1(x,t) + \tilde{u}_2(x,t) \\
 &= U_1 e^{i\left(\frac{\pi}{\ell_1} x - \omega t\right)} + U_2 e^{i\left(\frac{\pi}{\ell_2} x + \omega t\right)}
 \end{aligned} \tag{23}$$

where the constants W_1 , W_2 , U_1 , and U_2 can be readily determined by the substitution of Equation (23) into Equation (16). The radial response of the shell consists

$$\begin{aligned}
 \tilde{w}_1 &\equiv \frac{\rho_0 \omega \left(1 - \frac{V\pi}{\omega \ell_1}\right) \Phi_1(a) i A e^{i\left(\frac{\pi}{\ell_1} x - \omega t\right)}}{K\left(\frac{\pi}{\ell_1}\right)^4 + \frac{D}{a^2} - m\omega^2 - \frac{\left(\frac{\pi}{\ell_1}\right)^2 \left(\frac{\nu}{a} D\right)^2}{D\left(\frac{\pi}{\ell_1}\right)^2 - m\omega^2}} \\
 \tilde{w}_2 &\equiv \frac{-\rho_0 \omega \left(1 + \frac{Y\pi}{\omega \ell_2}\right) \Phi_2(a) i B e^{i\left(\frac{\pi}{\ell_2} x + \omega t\right)}}{K\left(\frac{\pi}{\ell_2}\right)^4 + \frac{D}{a^2} - m\omega^2 - \frac{\left(\frac{\pi}{\ell_2}\right)^2 \left(\frac{\nu}{a} D\right)^2}{D\left(\frac{\pi}{\ell_2}\right)^2 - m\omega^2}}
 \end{aligned} \tag{24}$$

The corresponding longitudinal response of the shell is



$$u(x,t) = \frac{\left(\frac{\pi}{\ell_1}\right) \left(\frac{v}{a}\right)^D i \tilde{w}_1}{D \left(\frac{\pi}{\ell_1}\right)^2 - m\omega^2} + \frac{\left(\frac{\pi}{\ell_2}\right) \left(\frac{v}{a}\right)^D i \tilde{w}_2}{D \left(\frac{\pi}{\ell_2}\right)^2 - m\omega^2} \quad (25)$$

Finally, substitution of the pertinent partial derivatives of Equations (17) and (23) into the boundary condition, Equation (15) - that is,

$$v_r(a,x,t) = \left. \frac{\partial \phi}{\partial r} \right|_{r=a} = \frac{\partial w}{\partial t} + v \frac{\partial w}{\partial x}$$

yields

$$f_1(\omega, \ell_1) A e^{i\left(\frac{\pi}{\ell_1} x - \omega t\right)} + f_2(\omega, \ell_2) B e^{i\left(\frac{\pi}{\ell_2} x + \omega t\right)} = 0$$

where

$$f_1 \equiv \Phi_1'(a) - \frac{\rho_0 \omega^2 \left(1 - \frac{V\pi}{\omega \ell_1}\right)^2 \Phi_1(a)}{K \left(\frac{\pi}{\ell_1}\right)^4 + \frac{D}{a^2} - m\omega^2 - \frac{\left(\frac{\pi}{\ell_1} \frac{v}{a} D\right)^2}{D \left(\frac{\pi}{\ell_1}\right)^2 - m\omega^2}}$$

$$f_2 \equiv \Phi_2'(a) - \frac{\rho_0 \omega^2 \left(1 + \frac{V\pi}{\omega \ell_1}\right)^2 \Phi_1(a)}{K \left(\frac{\pi}{\ell_2}\right)^4 + \frac{D}{a^2} - m\omega^2 - \frac{\left(\frac{\pi}{\ell_2} \frac{v}{a} D\right)^2}{D \left(\frac{\pi}{\ell_2}\right)^2 - m\omega^2}}$$



Consequently, for $A \neq 0$

$$f_1(\omega, \ell_1) = 0 \quad (26)$$

and, for $B \neq 0$

$$f_2(\omega, \ell_2) = 0 \quad (27)$$

Equations (26) and (27) are the characteristic equations of the downstream and the upstream-directed propagating waves, respectively, and they provide the frequency-wavelength or the phase velocity vs wave number relationships of the two waves. As occurred earlier with Equations (19) and (20), the analytical forms of $f_1(\omega, \ell_1)$ and $f_2(\omega, \ell_2)$ are also nearly identical. The essential difference between these two analytical functions, as before with Equations (19) and (20), depends on the ratios of the steady-state velocity V to the respective phase velocities, \tilde{v}_1 and \tilde{v}_2 . Since as much practical information as obtained from Equations (26) and (27) can be obtained from a simplified approximation of these equations, Equations (26) and (27) will not be examined further.

For most practical applications, the phase velocity of the propagating pressure wave reflecting essentially the fluid acoustic behavior is quite high and the steady-state flow velocity of the fluid, by contrast, is quite low. Consequently, the conditions

$$\frac{V}{\tilde{v}_1} = \frac{V\pi}{\omega\ell_1} \ll 1, \quad \frac{V}{\tilde{v}_2} = \frac{V\pi}{\omega\ell_2} \ll 1$$

describe appropriately the physical situation occurring in practical applications and the response of the propagating waves are established, with no appreciable inaccuracies, by the simplified approximation of Equations (26) and (27)

$$\Phi'(a) - \frac{\rho_0 \omega^2 \Phi(a)}{K\left(\frac{\pi}{\ell}\right)^4 + \frac{D}{a^2} - m\omega^2 - \frac{\left(\frac{\pi}{\ell} \frac{v}{a} D\right)^2}{D\left(\frac{\pi}{\ell}\right)^2 - m\omega^2}} = 0 \quad (28)$$



where

$$l \equiv l_1 \cong l_2$$

and

$$\Phi(r) \equiv \begin{cases} I_0(\alpha r), \alpha(\text{real}) \equiv \sqrt{\left(\frac{\pi}{l}\right)^2 - \left(\frac{\omega}{c}\right)^2} \\ J_0(\beta r), \beta(\text{real}) \equiv \sqrt{\left(\frac{\omega}{c}\right)^2 - \left(\frac{\pi}{l}\right)^2} \end{cases}$$

The corresponding properties of the response are, for the fluid pressures,

$$p(r,x,t) = \rho_0 \omega \begin{Bmatrix} I_0(\alpha r) \\ J_0(\beta r) \end{Bmatrix} \begin{pmatrix} i A e^{i\left(\frac{\pi}{l} x - \omega t\right)} & i\left(\frac{\pi}{l} x + \omega t\right) \\ - i B e^{i\left(\frac{\pi}{l} x + \omega t\right)} & \end{pmatrix} \quad (29)$$

For the fluid velocity components,

$$v_r(r,x,t) = \begin{Bmatrix} I_0'(\alpha r) \\ J_0'(\beta r) \end{Bmatrix} \left(A e^{i\left(\frac{\pi}{l} x - \omega t\right)} + B e^{i\left(\frac{\pi}{l} x + \omega t\right)} \right) \quad (30)$$

$$v(r,x,t) = \frac{\pi}{l} \begin{Bmatrix} I_0(\alpha r) \\ J_0(\beta r) \end{Bmatrix} \begin{pmatrix} i A e^{i\left(\frac{\pi}{l} x - \omega t\right)} & i\left(\frac{\pi}{l} x + \omega t\right) \\ i B e^{i\left(\frac{\pi}{l} x + \omega t\right)} & \end{pmatrix} \quad (31)$$



and, for the shell wall response, using also Equation (28),

$$w(x,t) = \frac{1}{\omega} \begin{Bmatrix} I_0'(\alpha a) \\ J_0'(\beta a) \end{Bmatrix} \begin{pmatrix} i \left(\frac{\pi}{\ell} x - \omega t \right) & i \left(\frac{\pi}{\ell} x + \omega t \right) \\ i A e & - i B e \end{pmatrix} \quad (32)$$

$$u(x,t) = \frac{\left(\frac{\pi}{\ell} \frac{v}{a} D \right)}{D \left(\frac{\pi}{\ell} \right)^2 - m\omega^2} \cdot i w(x,t) \quad (33)$$

where

$$I_0'(\alpha r) = \alpha I_1(\alpha r), \quad J_0'(\beta r) = -\beta J_1(\beta r)$$

Finally, it is to be noted that the quotient of Equation (29), evaluated at $r = a$, and Equation (32) yields

$$\frac{p(a,x,t)}{2(x,t)} = \omega^2 \rho_0 a \begin{Bmatrix} \frac{I_0(\alpha a)}{\alpha a I_1(\alpha a)} \\ - \frac{J_0(\beta a)}{\beta a J_1(\beta a)} \end{Bmatrix} \quad (34)$$

The term on the right-hand side of Equation (34) divided by ω^2 represents the apparent mass of the fluid.



EXAMINATION OF THE CHARACTERISTIC EQUATION

Equation (28) defines the frequency-wavelength relationship of the approximate standing wave, free harmonic, behavior of the coupled fluid and shell perturbations. It also establishes the phase velocity vs wave number relationship approximated to be the same for both the downstream and the upstream propagating waves.

It is convenient to reduce Equation (28) into a dimensionless equation containing only dimensionless parameters of the fluid/shell system. The appropriate parameters of the response are

$$\lambda^2 \equiv \left(\frac{\omega a}{c}\right)^2 \quad \text{and} \quad \kappa^2 \equiv \left(\frac{\pi a}{\ell}\right)^2 \quad (35)$$

designating dimensionless frequency and wave number parameters, respectively. The square of the ratio of the phase velocity to the fluid acoustic velocity is

$$\left(\frac{\tilde{v}}{c}\right)^2 = \left(\frac{\omega \ell}{\pi c}\right)^2 = \frac{\lambda^2}{\kappa^2} \quad (36)$$

The appropriate physical parameters of the fluid/shell system are

$$\left. \begin{aligned} \mu &\equiv \frac{\sigma^a}{m} \\ \sigma &\equiv \frac{mc^2}{D} = \left(\frac{c}{c_s}\right)^2 (1-\nu^2), & c_s^2 &= \frac{E}{\rho_s} \\ \epsilon &\equiv \frac{k}{a^2 D} = \frac{1}{12} \left(\frac{h}{a}\right)^2 \end{aligned} \right\} \quad (37)$$

where μ , σ and ϵ reflect the fluid-to-shell mass ratio, the square of the ratio of the fluid acoustic velocity to the shell elastic wave velocity, and the ratio of the shell wall bending rigidity to the shell wall extensional rigidity, respectively. One additional parameter, significant to the study, is



$$2\mu\sigma = \frac{B}{E} \frac{2a}{h} (1-v^2) \quad (38)$$

This parameter, for all practical purposes - that is, for the small practical values of Poisson's ratio, v - is the only term in addition to the acoustic velocity governing the phase velocity as described by the one-dimensional water hammer theory (cf., Equation 1). It is readily shown that Equation (28) in terms of these parameters is equivalent to the dimensionless equation,

$$\left(\epsilon \kappa^4 + 1 - \sigma \lambda^2 \right) - \frac{v^2 \kappa^2}{\kappa^2 - \sigma \lambda^2} = \mu \sigma^2 \frac{\Phi(a)}{a \Phi'(a)} \quad (39)$$

where

$$\frac{\Phi(a)}{a \Phi'(a)} = \begin{cases} \frac{I_0(\alpha a)}{\alpha a I_1(\alpha a)}, & \alpha a(\text{real}) \equiv \sqrt{\kappa^2 - \lambda^2} \\ \frac{-J_0(\beta a)}{\beta a J_1(\beta a)}, & \beta a(\text{real}) \equiv \sqrt{\lambda^2 - \kappa^2} \end{cases}$$

Before going into the general solution of Equation (39), it is useful to draw attention to the several qualitative features of the fluid/shell behavior that are immediately apparent. For example, it is apparent in Equation (39) that the coupling between the fluid and the shell depends on the value of the mass parameter, μ . If μ is large, as it normally is for a liquid and a thin-walled shell, the fluid/shell coupling is large. If μ is small, as it is for a liquid and a thick-walled shell, the fluid/shell coupling is small, and if μ is zero, Equation (39) pertains to the shell without the fluid. Moreover, by rewriting Equation (39) to read

$$\left\{ \epsilon \kappa^4 + 1 - \sigma \lambda^2 \left(1 + \mu \frac{\Phi(a)}{a \Phi'(a)} \right) \right\} - \frac{v^2 \kappa^2}{\kappa^2 - \sigma \lambda^2} = 0$$

It is apparent that the fluid/shell interaction exhibited by the terms in the parentheses involves only the shell radial behavior interacting with the fluid behavior. Regardless of the nature of the fluid pressures generated at the shell wall, the shell longitudinal behavior, reflected by the response



$$\kappa^2 - \sigma\lambda^2 = 0$$

or

$$\frac{\lambda^2}{\kappa^2} = \left(\frac{\tilde{v}}{c}\right)^2 = \frac{1}{\sigma} = \left(\frac{c_s}{c}\right)^2 (1-\nu^2)^{-1}$$

does not interact directly with the fluid but is coupled to the rest of the system by the shell wall extensional effects attributable to the Poisson's ratio, ν . This coupling, for most practical shells, is a weak and therefore is significant only for those values of frequencies and wavelengths satisfying simultaneously the two equations

$$\left\{ \begin{array}{l} \epsilon\kappa^4 + 1 - \sigma\lambda^2 \\ 1 + \mu \frac{\Phi(a)}{a \Phi'(a)} \end{array} \right\} = 0 \quad (40)$$

and

$$\kappa^2 - \sigma\lambda^2 = 0 \quad (41)$$

Furthermore, for the values of frequencies and wavelengths where this is not true, Equations (40) and (41) taken together represent a fair approximation of Equation (39).

Finally, as suggested by Equations (34) and (40), the nature of the pressures exhibited in the fluid is either subsonic or supersonic depending on whether or not

$$\frac{\lambda^2}{\kappa^2} = \left(\frac{\tilde{v}}{c}\right)^2 < 1$$

On the one hand, for $\lambda^2 > \kappa^2$, the phase velocities of the hydroelastic propagating waves are less than the fluid acoustic velocity. As suggested by both the sign and the diminishing intensity of the shell wall loading term,



$$\mu \frac{\Phi(a)}{a \Phi'(a)} = \mu \frac{I_0(\alpha a)}{\alpha a I_1(\alpha a)}, \quad \alpha a \equiv \sqrt{\kappa^2 - \lambda^2}$$

The pressures generated in the fluid are subsonic in nature. On the other hand, for $\lambda^2 > \kappa^2$, the phase velocities of the hydroelastic propagating waves are greater than the fluid acoustic velocity. As suggested by both the sign and the changing intensity of the shell wall loading term,

$$\mu \frac{\Phi(a)}{a \Phi'(a)} = - \frac{J_0(\beta a)}{\beta a J_1(\beta a)}, \quad \beta a \equiv \sqrt{\lambda^2 - \kappa^2}$$

The pressures generated in the fluid are supersonic in nature and exhibit complicated patterns in the fluid caused by the mutual interference of the generated acoustic waves. Actually, the steady-state flow velocity contributes to the velocity relative to the fluid of the hydroelastic propagating wave and, as shown by Equations (19) and (20), should be included. However, for small V , the sonic conditions for the two waves are nearly alike and are so treated. The shell wall loading characteristic of the propagating waves having subsonic and supersonic phase velocities is depicted in Figure 2.

Equation (39) is solved in two parts. The first part establishes the properties of the propagating waves having phase velocities less than the acoustic velocity. The second part deals with the propagating waves having phase velocities greater than the acoustic velocity.

The Properties of the Propagating Waves Having Subsonic Phase Velocities,

$$\lambda^2 \leq \kappa^2$$

Equation (39), for waves of subsonic phase velocities, is

$$\epsilon \kappa^4 + 1 - \sigma \lambda^2 \left\{ 1 + \mu \frac{I_0(\alpha a)}{\alpha a I_1(\alpha a)} \right\} - \frac{v^2 \kappa^2}{\kappa^2 - \sigma \lambda^2} = 0 \quad (42)$$

where

$$\alpha a \equiv \sqrt{\kappa^2 - \lambda^2}$$



It is convenient to introduce a change of variables - that is

$$\eta^2 = \kappa^2 - \lambda^2 \geq 0, \quad \lambda^2 = \kappa^2 - \eta^2$$

Expressed in terms of the new variable, Equation (42), with additional algebraic manipulation, is readily shown to be equivalent to

$$\psi_1(\eta^2) = Y(\eta^2) \tag{43}$$

where

$$\psi_1(\eta^2) \equiv \frac{1}{1 + \mu \frac{I_0(\eta)}{\eta I_1(\eta)}}$$

$$Y(\eta^2) \equiv \frac{(\kappa^2 - \eta^2) \left[\eta^2 + \left(\frac{1}{\sigma} - 1 \right) \kappa^2 \right]}{\left(\frac{\epsilon}{\sigma} \kappa^4 + \frac{1}{\sigma} \right) \left[\eta^2 + \left(\frac{1}{\sigma} - 1 \right) \kappa^2 \right] - \left(\frac{\nu}{\sigma} \right)^2 \kappa^2}$$

Since both $\psi_1(\eta^2)$ and $Y(\eta^2)$ are easily calculated, for prescribed values of κ^2 , Equation (43) as depicted in Figure 3, may be solved graphically for the corresponding values of η^2 satisfying the identity. Both $\psi_1(\eta^2)$ and $Y(\eta^2)$ behave monotonically with respect to η^2 . Near the origin, $\psi_1(\eta^2)$ behaves in accordance with the series.

$$\psi_1(\eta^2) = \frac{1}{2\mu} \eta^2 - \frac{1}{4\mu} \left(\frac{1}{4} + \frac{1}{\mu} \right) \eta^4 + \frac{1}{8\mu} \left(\frac{1}{12} + \frac{1}{2\mu} + \frac{1}{\mu^2} \right) \eta^6 - \dots \tag{44}$$

For large values of η^2 , $\psi_1(\eta^2)$ behaves in accordance with

$$\lim_{\eta^2 \rightarrow \infty} \psi_1(\eta^2) = \lim_{\eta^2 \rightarrow \infty} \left(\frac{1}{1 + \frac{\mu}{\eta}} \right) = 1$$



and, regardless of the value of η^2 , the value of $\psi_1(\eta^2)$ never exceeds one. The function $Y(\eta^2)$, on the other hand, is more complicated but nevertheless also easily managed. As shown in Figure 3, the descriptive features of $Y(\eta^2)$ include, for $Y(\eta_o^2) = 0$,

$$\eta_o^2 = -\left(\frac{1}{\sigma} - 1\right)\kappa^2 \quad \text{and} \quad \eta_o^2 = \kappa^2$$

For $Y(\eta_p^2) = \infty$,

$$\eta_p^2 = -\left(\frac{1}{\sigma} - 1\right)\kappa^2 + \frac{\left(\frac{v}{\sigma}\right)^2 \kappa^2}{\frac{\epsilon}{\sigma} \kappa^4 + \frac{1}{\sigma}}$$

and, for the Y-axis intercept,

$$Y(0) = \frac{\left(\frac{1}{\sigma} - 1\right)\kappa^2}{\left(\frac{1}{\sigma} - 1\right)\left(\frac{\epsilon}{\sigma} \kappa^4 + \frac{1}{\sigma}\right) - \left(\frac{v}{\sigma}\right)^2}$$

It is apparent in Figure 3 that the general nature of the solution of Equation (43) depends on the value of the parameter

$$\frac{1}{\sigma} \equiv \left(\frac{c_s}{c}\right)^2 (1-v^2)^{-1}$$

which normally, for practical shells and fluids, is always greater than one. In this case, Equation (43) yields only one set of values of η^2 for the corresponding set of values of κ^2 . On the otherhand, for $\frac{1}{\sigma} < 1$, it is apparent that Equation (43) yields two sets of values of η^2 . Consequently, no more than two solutions reflecting the frequency wavelength properties of two modes of behavior are admitted by Equation (43). However, due to the fact that normally, $\frac{1}{\sigma} > 1$, Equation (43), for most practical applications, admits only one. An approximate analytical solution of this low frequency branch is easily determined.



For the wave behavior of wavelengths longer than the transition wavelengths (cf., Equation 3), the bending rigidity term, $\epsilon \kappa^4$, in Equation (43) can be ignored and Equation (43) can be algebraically manipulated to yield

$$\left(\frac{1}{\sigma} - 1\right) \frac{\kappa^4}{\eta^4} + \left\{ 1 - \left(\frac{1}{\sigma} - 1\right) \left(1 + \frac{\psi_1}{\eta^2 \sigma}\right) + \nu^2 \frac{\psi_1}{\eta^2 \sigma^2} \right\} \frac{\kappa^2}{\eta^2} - \left(1 + \frac{\psi_1}{\eta^2 \sigma}\right) = 0$$

This equation represents a quadratic equation involving the unknown, $\frac{\kappa^2}{\eta^2}$. Its solution is

$$\frac{\kappa^2}{\eta^2} \cong \frac{1 - \left(\frac{1}{\sigma} - 1\right) \left(1 + \frac{\psi_1}{\eta^2 \sigma}\right) + \nu^2 \frac{\psi_1}{\eta^2 \sigma^2}}{2\left(\frac{1}{\sigma} - 1\right)} \pm \frac{\sqrt{\left\{ 1 - \left(\frac{1}{\sigma} - 1\right) \left(1 + \frac{\psi_1}{\eta^2 \sigma}\right) + \eta^2 \frac{\psi_1}{\eta^2 \sigma^2} \right\}^2 + 4\left(\frac{1}{\sigma} - 1\right) \left(1 + \frac{\psi_1}{\eta^2 \sigma}\right)}}{2\left(\frac{1}{\sigma} - 1\right)}$$

(45)

where it is important to note that

$$\lim_{\eta^2 \rightarrow 0} \left(\frac{\psi_1}{\eta^2 \sigma} \right) = \frac{1}{2\mu\sigma}$$

Only, the positive values of κ^2 for $\eta^2 \geq 0$ are significant, physically. Consequently, for the practical case where $\frac{1}{\sigma} > 1$, the negative sign of the radical expression of Equation (45) is to be ignored. Equation (45) yields the relationship,

$$\frac{\kappa^2}{\eta^2} = f(\eta^2)$$



This relationship, in turn, yields

$$\left. \begin{aligned} \lambda^2 &= \kappa^2 - \eta^2 = \left\{ f(\eta^2) - 1 \right\} (\eta^2) \\ \kappa^2 &= f(\eta^2) \cdot (\eta^2) \end{aligned} \right\} \quad (46)$$

That is, a pair of parametric equations having the parameter, η^2 . Equation (46) describes the frequency-wavelength relationship of the low frequency mode for the wave behavior of wavelengths longer than the transition wavelength.

For the wave behavior characterized by wavelengths equal to and shorter than the transition wavelength (c.f., Equation (3)), the bending rigidity term, $\epsilon\kappa^4$, appearing in Equation (43) must be retained. It is suggested by the preceding examination of Equation (43) that the first branch solution for large values of κ^2 is

$$\eta^2 \approx \kappa^2$$

Substitution of the corresponding approximations,

$$\alpha a \approx \kappa \quad \text{and} \quad \sigma \lambda^2 - \kappa^2 \approx -\kappa^2$$

into Equation (42) yields

$$\lambda^2 \cong \frac{1}{\sigma} \left\{ \frac{1 - v^2 + \epsilon\kappa^4}{1 + \mu \frac{I_0(\kappa)}{I_1(\kappa)}} \right\} \quad (47)$$

or, after substituting Equations (35) and (37)

$$\omega^2 \cong \frac{\frac{D}{a^2} (1 - v^2 + \epsilon\kappa^4)}{m \left\{ 1 + \mu \frac{I_0(\kappa)}{\kappa I_1(\kappa)} \right\}}$$



Equation (47), an approximation for the wave behavior of very short wavelengths, is recognized to reflect shell wall radial behavior modified by the apparent mass of the fluid. As $\kappa \rightarrow \infty$, the intensity of the apparent mass of the fluid diminishes and, consistent with the theory of subsonic hydrodynamics, only the fluid immediately localized to the shell wall interacts with it. The development of Equations (43), (45), (46) and (47) should conclude the examination of Equation (42). However, one more task remains.

It is important to show that the first branch solution for wave behavior of only very long wavelengths or very small wave numbers tends to agree with the solution described by the one-dimensional water hammer theory and that only in the limiting case for $\ell \rightarrow \infty$ or $\kappa \rightarrow 0$, do the two theories for negligible effects of Poisson's ratio, yield the same result. This can be accomplished by reducing Equation (43) for $\eta^2 \rightarrow 0$ and $\kappa^2 \rightarrow 0$. However, since for $\kappa^2 \rightarrow 0$ the bending rigidity term $\epsilon \kappa^4$ is not significant, this can also be accomplished using Equations (45) and (46). The term under the radical of Equation (45) is equivalent to

$$\left\{ 1 + \left(\frac{1}{\sigma} - 1 \right) \left(1 + \frac{\psi_1}{\eta^2 \sigma} \right) \right\} + 2\nu^2 \frac{\psi_1}{\eta^2 \sigma^2} \left\{ 1 - \left(\frac{1}{\sigma} - 1 \right) \left(1 + \frac{\psi_1}{\eta^2 \sigma} \right) \right\}$$

For practical shells having small Poisson's ratio effects and practical liquids, the value of the second group of terms is several times smaller than the value of the first group of terms. Consequently, the radical expression of Equation (45) can be approximated by

$$\sqrt{\left\{ 1 - \left(\frac{1}{\sigma} - 1 \right) \left(1 + \frac{\psi_1}{\eta^2 \sigma} \right) + \nu^2 \frac{\psi_1}{\eta^2 \sigma^2} \right\}^2 + 4 \left(\frac{1}{\sigma} - 1 \right) \left(1 + \frac{\psi_1}{\eta^2 \sigma} \right)}$$

$$\cong 1 + \left(\frac{1}{\sigma} - 1 \right) \left(1 + \frac{\psi_1}{\eta^2 \sigma} \right) + \nu^2 \frac{\psi_1}{\eta^2 \sigma^2} \left\{ \frac{1 - \left(\frac{1}{\sigma} - 1 \right) \left(1 + \frac{\psi_1}{\eta^2 \sigma} \right)}{1 + \left(\frac{1}{\sigma} - 1 \right) \left(1 + \frac{\psi_1}{\eta^2 \sigma} \right)} \right\}$$

It follows, in accordance with Equation (45), that



$$\frac{\kappa^2}{\eta^2} \cong f(\eta^2)$$

$$\cong 1 \left(+ \frac{\psi_1}{\eta^2 \sigma} \right) \left\{ 1 - \frac{v^2}{\sigma} \cdot \frac{\frac{\psi_1}{\eta^2 \sigma}}{1 + \left(\frac{1}{\sigma} - 1 \right) \left(1 + \frac{\psi_1}{\eta^2 \sigma} \right)} \right\} \quad (48)$$

Substitution of Equation (48) into Equation (46)

$$\frac{\lambda^2}{\eta^2} \cong \frac{\psi_1}{\eta^2 \sigma} \left\{ 1 - \frac{v^2}{\sigma} \cdot \frac{1 + \frac{\psi_1}{\eta^2 \sigma}}{1 + \left(\frac{1}{\sigma} - 1 \right) \left(1 + \frac{\psi_1}{\eta^2 \sigma} \right)} \right\} \quad (49)$$

Equations (48) and (49) are a pair of parametric equations, expressing approximately the first branch function of λ^2 in terms of the parameter η^2 . These equations which are easier to work with may be used in place of Equations (45) and (46). The quotient, dividing Equation (49) by Equation (48), is, approximately,

$$\frac{\lambda^2}{\kappa^2} \cong \frac{\frac{\psi_1}{\eta^2 \sigma}}{1 + \frac{\psi_1}{\eta^2 \sigma}} \left\{ 1 - \frac{v^2}{\sigma} \cdot \frac{1}{1 + \left(\frac{1}{\sigma} - 1 \right) \left(1 + \frac{\psi_1}{\eta^2 \sigma} \right)} \right\}$$

Finally, it follows from Equation (44) that

$$\frac{\psi_1}{\eta^2 \sigma} = \frac{1}{2\mu\sigma} \left\{ 1 - \frac{1}{2} \left(\frac{1}{4} - \frac{1}{\mu} \right) \eta^2 + \dots \right\}$$



Therefore, for $v^2 \approx 0$,

$$\lim_{\substack{\eta^2 \rightarrow 0 \\ \kappa^2 \rightarrow 0}} \left(\frac{\lambda^2}{\kappa^2} \right) \cong \frac{1}{1 + 2\mu\sigma} \cong \frac{1}{1 + \frac{B}{E} \frac{2a}{h}}$$

It is apparent that Equation (50) agrees with Equation (1). However, this agreement occurs only in the limiting case where $\kappa^2 \rightarrow 0$ and for $v^2 \approx 0$.

The Properties of the Propagating Waves Having Supersonic Phase Velocities
 $\lambda^2 \geq \kappa^2$

Equation (39), for waves of supersonic phase velocities is

$$\epsilon \kappa^4 + 1 - \sigma \lambda^2 \left\{ 1 - \mu \frac{J_0(\beta a)}{\beta a J_1(\beta a)} \right\} - \frac{v^2 \kappa^2}{\kappa^2 - \sigma \lambda^2} = 0 \quad (51)$$

where

$$\beta a \equiv \sqrt{\lambda^2 - \kappa^2}$$

Again, it is convenient to introduce a change of variables - that is,

$$\zeta^2 = \lambda^2 - \kappa^2, \quad \lambda^2 = \kappa^2 + \zeta^2$$

Expressed in terms of the new variable, Equation (51) with additional algebraic manipulation is readily shown to be equivalent to



$$\psi_2(\zeta^2) = \frac{(\kappa^2 + \zeta^2) \left[\zeta^2 - \left(\frac{1}{\sigma} - 1 \right) \kappa^2 \right]}{\left(\frac{\epsilon}{\sigma} \kappa^4 + \frac{1}{\sigma} \right) \left[\zeta^2 - \left(\frac{1}{\sigma} - 1 \right) \kappa^2 \right] + \left(\frac{\nu}{\sigma} \right)^2 \kappa^2} \quad (52)$$

where

$$\psi_2(\zeta^2) \equiv \frac{1}{1 - \mu \frac{J_0(\zeta)}{\zeta J_1(\zeta)}}$$

Equation (52) cannot be solved analytically. Moreover, due to the fact that $\psi_2(\zeta^2)$ exhibits singularities, the approximate analytical procedures used in the preceding section are useless. The only procedure likely to be successful is a graphic one.

Equation (52) can be rearranged to describe the identity,

$$\frac{1}{\zeta^2 \sigma} \psi_2(\zeta^2) = G\left(\frac{\kappa^2}{\zeta^2}\right) \quad (53)$$

where

$$G \frac{\kappa^2}{\zeta^2} \equiv \frac{\left(1 + \frac{\kappa^2}{\zeta^2} \right) \left(\frac{\sigma}{\sigma-1} + \frac{\kappa^2}{\zeta^2} \right)}{\frac{\sigma}{\sigma-1} + \left(1 + \frac{\nu^2}{\sigma-1} \right) \frac{\kappa^2}{\zeta^2}}$$

Since in the high frequency regime of supersonic phase velocities the bending rigidity term, $\epsilon \kappa^4$, is negligible, it is ignored in Equation (53). The purpose of Equation (53) is to establish the relationship between the argument of the term on the right side, κ^2/ζ^2 , and the argument of the term on the left-hand side, ζ^2 , satisfying the identity. Having established this relationship - say, $g(\zeta^2)$ - the two relationships

$$\left. \begin{aligned} \lambda^2 &= \kappa^2 + \zeta^2 = \left\{ g(\zeta^2) + 1 \right\} \zeta^2 \\ \kappa^2 &= g(\zeta^2) \cdot \zeta^2 \end{aligned} \right\} \quad (54)$$



are readily calculated. Equation (54) provides a pair of parametric equations of the parameter, ζ^2 , that describe the frequency-wavelength relationship of the high frequency modes of behavior.

The term on the left-hand side of Equation (53) is readily evaluated for selected values of σ and μ . Its analytical behavior near the origin is

$$\frac{1}{\zeta^2 \sigma} \psi_2(\zeta^2) = -\frac{1}{2\mu\sigma} - \frac{1}{4\mu\sigma} \left(\frac{1}{4} + \frac{1}{\mu} \right) \zeta^2 - \frac{1}{8\mu\sigma} \left(\frac{1}{12} + \frac{1}{2\mu} + \frac{1}{\mu^2} \right) \zeta^4 - \dots \quad (55)$$

The other pertinent analytical features include (1) the infinite number of zeros established by

$$J_1(\zeta_0) = 0, \quad \zeta_0 \neq 0 \quad (56)$$

That is,

$$(\zeta_0^2)_n = 14.69, 49.1, 103.4, 177.0, \dots$$

and (2) the infinite number of singularities established by

$$\frac{\zeta_p}{\mu} = \frac{J_0(\zeta_p)}{J_1(\zeta_p)} \quad (57)$$

These features, typical of the term on the left-hand side of Equation (53), are depicted in Figure 4.

The term on the right-hand side of Equation (53) is also readily evaluated for selected values of σ and v^2 . The pertinent descriptive features of G include, for the G -axis intercept,

$$G(0) = 1$$

for $G = 0$, the zeros,



$$\left(\frac{\kappa^2}{\zeta^2}\right)_0 = -1$$

$$\left(\frac{\kappa^2}{\zeta^2}\right)_0 = \frac{\sigma}{1-\sigma}$$

For $G = \infty$, the singularity

$$\left(\frac{\kappa^2}{\zeta^2}\right)_p = \frac{\sigma}{1-\sigma-v^2}$$

and, for the locations of the zero slope of G ,

$$\left(\frac{\kappa^2}{\zeta^2}\right)_{\text{zero slope}} = \frac{\sigma \pm v \sqrt{\frac{\sigma}{1-\sigma}(1-v^2)}}{1-\sigma-v^2}$$

Other particular slopes of G are

$$G'(-1) = \frac{1}{1-v^2}$$

$$G'(0) = 1 - \frac{v^2}{\sigma}$$

$$G'\left(\frac{\sigma}{1-\sigma}\right) = -\frac{1}{v^2} \left(\frac{1-\sigma}{\sigma}\right)$$

The features typical of the term on the right-hand side of Equation (53) are depicted in Figure 5. If $(\sigma + v^2) < 1$, the singularity of G will appear to the right of the origin as shown in Figure 5. If $(\sigma + v^2) > 1$, the singularity of G will appear to the left of the origin, leaving a smooth unbroken curve to the right. The position of the singularity of G , as will be demonstrated shortly, has no real physical significance.

Once the terms on both sides of Equation (53) are evaluated, the relationship

$$\frac{\kappa^2}{\zeta^2} = g(\zeta^2)$$



instrumental to the solution is readily determined. An infinite number of branches of this relationship are generated. The point by point mapping of this relationship, for the various branches, is depicted in Figure 6. The arrows and the consecutively numbered points show how the first branch of $g(\zeta^2)$ is generated. Although the mapping shown in this figure suggests graphic construction, it is not intended that graphic construction be used. The primary purpose of Figure 6 is to depict the nature of the one-to-one correspondence reflected by Equation (53), for each branch of $g(\zeta^2)$ generated.

For example, it is apparent in Figure 6 that the singularities of the terms on both sides of Equation (53), for instance, denoted by points (3) and (4) do not represent singularities of the mapped function, $g(\zeta^2)$. On the other hand, the singularities of $(\psi_2/\zeta^2\sigma)$, denoted approximately by the points (6) and (16) in Figure 6, map as the vertical asymptotes of $g(\zeta^2)$. These vertical asymptotes, defined by the equation $\zeta^2 = \zeta_{p_n}^2$, and established in value by Equation (57), in turn, as shown in Figure 7, appear in the λ^2, κ^2 - plane as the straight lines.

$$\lambda^2 = \zeta_{p_n}^2 + \kappa^2; \quad n = 1, 2, 3 \dots$$

Additional relationships between the branches of $g(\zeta^2)$ and the branches of $\lambda^2(\kappa^2)$ include the solution designated by point (10). For $\sigma < 1$, each supersonic branch includes such a point defined by

$$\left. \begin{aligned} \lambda_{(10)_n}^2 &= \left(\frac{\sigma}{1-\sigma} + 1 \right) \zeta_{o_n}^2 \\ \kappa_{(10)_n}^2 &= \left(\frac{\sigma}{1-\sigma} \right) \zeta_{o_n}^2 \end{aligned} \right\} \frac{\lambda_{(10)_n}^2}{\kappa_{(10)_n}^2} = \frac{1}{\sigma}$$

where, defined by Equation (56)

$$\zeta_{o_n}^2 = 14.69, 49.1, 103.4, 177.0, \dots$$



Furthermore, the zeros of $g(\zeta^2)$, for instance, denoted by point (7) in Figure 6, are the λ^2 -axis intercepts of the various branches. Finally, the slope at the origin of the first supersonic branch of $\lambda^2(\kappa^2)$ is related to the g -axis intercept - denoted by Point (1) in Figure 6 - in accordance with

$$\begin{aligned} \lim_{\kappa^2 \rightarrow 0} \left(\frac{\lambda^2}{\kappa^2} \right) &= \lim_{\zeta^2 \rightarrow 0} \left(\frac{g(0) + 1}{g(0)} \right) \\ &= \frac{1 + \Delta(1 - \sigma)}{\sigma + \Delta(1 - \sigma)} \end{aligned}$$

provided $g(0)$ exists. In most practical applications, $\sigma < 1$ and, therefore, the first supersonic branch of $\lambda^2(\kappa^2)$ passes through the origin and possesses the slope at the origin slightly less than $\frac{1}{\sigma}$. These properties are depicted in Figure 7. The development of Equation (53) and the subsequent discussion concludes the examination of Equation (51).



CALCULATED RESPONSE PROPERTIES TYPICAL OF THE FEED LINES
OF ROCKET PROPELLANT SYSTEMS

The calculation of the frequency-wavelength curves or the phase-velocity vs wavenumber curves is straightforward. Either Equation (43) or Equations (45), (46) and (47) or Equations (48), (49), and (47) define the branches for the propagating waves that are characterized by subsonic phase velocities. Equation (53), in conjunction with Equation (54), defines the branches for the propagating waves that are characterized by supersonic phase velocities. Finally, Equations (29) through (34) establish the corresponding modal response of the fluid and the shell. These calculations may be adapted to the digital computer but they are performed just as easily on the hand calculator.

Two cases, typical of the behavior of the propellant in the feed lines of rocket propellant systems, have been calculated and are reviewed below. The physical parameters representative of current rocket propellants and feed line materials are summarized in Table I. The parameter, μ , for a given ratio of wall thickness to cylinder radius, varies considerably depending on the propellant and the feed line material. However, the parameter σ , for a given propellant remains essentially constant for the various feed line materials reviewed. The two cases selected for examination are

1) LOX/7075-T6

$$c = 4,420 \text{ ft/sec}$$

$$\rho_0 g = 0.0413 \text{ lbs/in}^3$$

$$\frac{h}{a} = 10^{-2}$$

$$v^2 = 0.1089$$

$$\mu = 40.9$$

$$\sigma = 0.0571$$

$$B = 300,000 \text{ lbs/in}^2$$

2) LH₂/7075-T6

$$c = 17,730 \text{ ft/sec}$$



$$\begin{aligned} \rho_o g &= 0.00256 \text{ lbs/in}^3 \\ \frac{h}{a} &= 10^{-2} \\ v^2 &= 0.1089 \\ \mu &= 2.54 \\ \sigma &= 0.926 \\ B &= 300,000 \text{ lbs/in}^2 \end{aligned}$$

The preceding cases are selected as representative of current rocket propellant systems. Since the parameter σ does not vary significantly for the various feed line materials--aluminum, steel and titanium--the average value of σ for these materials is used. Poisson's ration ν , also varies but a few percent from material to material. The shell wall bending rigidity reflected by the parameter, ϵ , is important only when the wavelength of the response becomes as short as the transition wavelength (cf., Equation (3)). Consequently, the only parameter that can alter the response to any appreciable extent is the mass parameter, μ . The values of μ selected for the calculated cases are believed to be representative of the largest and the smallest values of practical interest.

The lower branch of the frequency-wavelength relationship characterized by phase velocities smaller than the acoustic velocity was calculated using (a) Equations (43), (b) Equations (45), (46) and (47), and (c) Equations (48), (49), and (47). The transition wave number, for $\frac{h}{a} = 10^{-2}$ is

$$\kappa_t^2 \equiv \left(\frac{\pi a}{\ell_t} \right)^2 = 337$$

(cf., Equation (3)). The calculated results for the two cases are presented in Figures 8 and 9. The graphical procedure, based on Equation (43), did not work well, due to the fact that $\eta^2 \approx \kappa^2$ over most of the solution and $\lambda^2 = \kappa^2 - \eta^2$. The solution η^2 cannot be generated precisely enough graphically for a meaningful difference, $\kappa^2 - \eta^2 = \lambda^2$, to be resolved. The alternate procedures, based on numerical calculations, yielded much better results. The calculations, made to compare Equations (45) and (48), revealed essentially the same numerical result.



The results depicted in Figures 8 and 9 are based on Equations (48) and (49). As indicated by Equation (50), the value of the curves at $\kappa^2 = 0$, shown in Figure 9, are identical to the result given by the one-dimensional water hammer theory. It is apparent that, for non-zero wave numbers, the phase velocity does not remain constant as suggested by the water hammer theory but decreases in magnitude as the wave number increases. In most practical applications, the primary concern is for the wave behavior of long wavelengths and, in such cases, the water hammer theory is applicable.

The higher branches of the frequency-wavelength relationship characterized by phase velocities larger than the acoustic velocity were calculated using the graphical procedure of Equation (53). The pertinent auxiliary curves of Equation (53) for the two cases are presented in Figures 10, 11, 12 and 13. The graphical solution of the supplementary equation, Equation (57), is presented in Figure 14. The final results for the two cases are presented in Figures 15 and 16. No difficulty in maintaining precision was encountered in this graphical solution.

The results depicted in Figures 15 and 16 include the response properties of the low frequency mode of behavior as well as the response properties of the high frequency acoustic modes of behavior. Figures 15b and 16b also show the response properties of the decoupled shell longitudinal behavior and the decoupled shell radial behavior. Consistent with the conclusion established in References 8 and 9, appreciable shell wall bending effects, disclosed by the curvature of the lower branch away from the κ^2 -axis, are not apparent for the wavelengths considered. Furthermore, due to the large value of μ coupling the fluid and the shell wall radial behavior, the properties of the coupled response depicted in Figure 15b are nowhere close to the properties of the decoupled shell radial behavior. For the case depicted in Figure 16b, where μ is considerably less, the properties of the coupled response tend to be much closer to the properties of the decoupled shell behavior. Finally, the coupling reflected by Poisson's ratio, ν , is weak as disclosed in Figures 15b and 16b by how well the higher branches of the coupled response duplicate the response curve of the uncoupled shell longitudinal behavior. The diagonally directed portions of the higher -ranch response curves for the coupled behavior reflect not the interaction between the fluid and the shell longitudinal behavior but the interaction between the fluid acoustic behavior and the shell radial behavior. Typical modal properties of the first branch and the diagonally directed portions of the higher branches are presented in Figure 17.



PRECEDING PAGE BLANK NOT FILMED.

CONCLUDING REMARKS AND RECOMMENDATIONS

The work completed and presented in this report shows that the coupled response properties of the hydroelastic propagating waves of a fluid-filled cylindrical shell reflect (1) strong direct coupling, depending on the parameter μ , between the fluid and the radial behavior of the shell and (2) weak indirect coupling, depending on the parameter, ν , between the fluid and the longitudinal behavior of the shell. The response properties, for most practical purposes, reflect coupled fluid and shell radial behavior. For the coupled fluid/shell modes of behavior, the nature of the pressures generated in the fluid depends on whether or not the hydroelastic wave velocity is greater or less than the acoustic velocity. On the one hand, the fluid behaves supersonically whereas, on the other hand, the fluid behaves subsonically. As shown in Figures 15 and 16, the modal frequencies of the subsonic branch are well separated from the modal frequencies of the supersonic branches.

The low frequency hydroelastic behavior characterized by subsonic phase velocities, for very long wavelengths relative to the radius of the cylinder, is essentially identical to the behavior represented by the one-dimensional water hammer theory. As shown in Figure 17a, the cross-sectional distributions of both the pressure and the longitudinal velocity perturbations, for this case, are essentially uniform. The corresponding radial distribution of the radial component of the fluid velocity perturbation is essentially a linear function of the radius, being zero at the cylinder axis and equal to the radial velocity of the shell wall at the shell wall.

The low frequency hydroelastic behavior characterized by subsonic phase velocities, for short wavelengths relative to the radius of the cylinder is primarily the response of just the shell wall, having only the fluid immediately adjacent to the shell wall responding with it. This behavior is governed by the physical properties of the shell and the apparent mass of the fluid in the proximity of the wall. The fluid pressures at the shell wall act opposite to the structural resistance of the shell. For exceedingly short wavelengths, the shell wall interaction with the fluid does not penetrate into the fluid at all.

The high frequency hydroelastic behavior characterized by supersonic phase velocities involves the multi-mode acoustic vibrations of the fluid coupled with the radial behavior of the shell wall. As shown in Figures 17b and 17c, large pressure and longitudinal velocity perturbations generated by the reinforcement of the acoustic waves reflected from the shell wall occur along the axis of the cylinder. Due to the interference of the acoustic waves, regimes of no pressure and velocity perturbations or, stated differently, nodes of the response, occur in the fluid. At the shell wall, the fluid pressures act in phase with the structural resistance of the cylinder.



In view of the response to excitation, the hydroelastic waves of low frequency and long wavelength are of primary concern. It is likely that this response is easily excited and is very lightly damped. For wavelengths approximately longer than the diameter of the shell, the behavior can be represented by the one-dimensional water hammer theory without introducing any appreciable errors. For impact type excitation both the low frequency behavior and the high frequency acoustic behavior are excited. However, without persistent high frequency excitation, the acoustic modes of behavior will damp out leaving just the low frequency quasi-plane wave response.

Since work on the present contract started in 1955, the following three problems of pressure wave propagation in fuel lines have been solved:

1. One-dimensional unsteady fluid motion in an elastic pipe was solved with various disturbance functions at the pump end. This formulation does not allow consideration of radial inertia in the shell or in the fluid. [Reference 3]
2. Two-dimensional viscous incompressible fluid flow in an elastic pipe was solved in the laminar flow region. This study does include the radial and longitudinal inertia of thin wall pipe, but it ignores bending stresses in the shell. [References 14 and 15]
3. Two-dimensional compressible inviscid fluid flow in an elastic pipe was solved for propagating harmonic waves in both the subsonic and supersonic regions. In this study the pipe is treated in accordance with the shell theory. The bending rigidity of the shell wall is included; however, the transverse shearing rigidity is ignored. [Present report]

The above program has fairly well covered the ground of investigation of pressure wave propagation in a single-phase fluid flow. Hence, it is the logical time to recommend the study of the dynamic effect of cavitating bubbles in the feed line as the continuation of the present effort. The importance of cavitation played in the self-induced longitudinal oscillation problem has been fully exemplified by experts in the Langley POGO meeting, February 1966. A general observation about this specific problem is that an understanding of methods to estimate the frequency in a cavitating fluid flow is not now available. Research on this fundamental and important ingredient, including nonlinear aspects, is indicated as necessary.

In view of the many unsurpassable difficulties associated with the cavitating flow problem physically and mathematically, it is suggested to investigate the following three tasks as the initial step for a study of cavitation effect on pressure wave propagation in a feed line:



- A. Formulate natural coordinates for axial-symmetric cavitating bubble.
- B. Determine the cavitation boundary in terms of geometric shape and its variation with time.
- C. Demonstrate the cavitating disturbances by a simple model.



PRECEDING PAGE BLANK NOT FILMED.

REFERENCES

- [1] Stenning, A. H. and J. L. Shearer, "Fundamentals of Fluid Flow," Fluid Power Control, edited by J. F. Blackburn, G. Reethof and J. L. Shearer, MIT Press, MIT, Cambridge, Mass., 1960.
- [2] Paynter, H. M., "Fluid Transients in Engineering Systems," Handbook of Fluid Dynamics, V. L. Streeter, Editor-in-Chief, McGraw-Hill Book Co., Inc., New York, 1961.
- [3] Fox, Edward C., "Feedline Flow," Rocket Propellant and Pressurization Systems, Edited by Elliott Ring, Prentice-Hall, Inc., Englewood Cliffs, New Jersey, 1964.
- [4] Fashbaugh, R. H., and V. L. Streeter, "Resonance in Liquid Rocket Engine System," Journal of Basic Engineering, December 1965.
- [5] Junger, M. C., "The Effect of a Surrounding Fluid on Pressure Waves in a Fluid Filled Elastic Tube," Journal of Applied Mechanics, June 1955.
- [6] Bleich, H. H. and M. L. Baron, "Free and Forced Vibrations of an Infinitely Long Cylindrical Shell in an Infinite Acoustic Medium," Journal of Applied Mechanics, March 1954.
- [7] Berry, J. G. and E. Reissner, "The Effect of an Internal Compressible Fluid Column on the Breathing Vibrations of a Thin Pressurized Cylindrical Shell," Journal of Aerospace Sciences, May 1958.
- [8] Herrmann, G., and I. Mirsky, "Three-Dimensional and Shell-Theory of Analysis of Axially Symmetric Motions of Cylinders," Journal of Applied Mechanics, December 1956.
- [9] Mirsky, I. and G. Herrmann, "Axially Symmetric Motions of Thick Cylindrical Shells," Journal of Applied Mechanics, March 1958.
- [10] "Handbook of Fluid Dynamics," V. L. Streeter, Editor-in-Chief, McGraw-Hill Book Co., Inc., New York, 1961.



- [11] Ashley, Holt, and Marten Landahl, "Aerodynamics of Wings and Bodies," Addison-Wesley Publishing Co., Inc., Reading, Mass., 1965.
- [12] Flügge, Wilhelm, "Stresses in Shells," Springer-Verlag, Berlin/Göttingen/Heidelberg, 1962.
- [13] Wing, H., and C. L. Tai, "One Dimensional Wave Propagation in a Feed Line," A Study of Longitudinal Oscillations of Propellant Tanks and Wave Propagations in Feed Lines, SID 66-46-1.
- [14] Loh, M. M. H., and C. L. Tai, "Wave Propagation in Elastic Pipe Filled with Incompressible Viscous Fluid," A Study of Longitudinal Oscillations of Propellant Tanks and Wave Propagations in Feed Lines, SID 66-46-2.
- [15] Fung, S. A., and C. L. Tai, "Wave Propagation in an Elastic Pipe Filled with Incompressible Viscous Streaming Fluid," A Study of Longitudinal Oscillations of Propellant Tanks and Wave Propagations in Feed Lines, SID-66-46-3.



TABLE 1.
TYPICAL PROPELLANT/DUCT PARAMETERS

Propellant Acoustic Velocities:

$$C_{LOX} = 4,420 \text{ ft/sec}$$

$$C_{LH_2} = 17,730 \text{ ft/sec}$$

Mass Parameter, $\mu \times \frac{h}{a} \equiv \frac{\rho}{\rho_s}$

| FLUID \ DUCT | ALUMINUM 7075-T6 | STEEL 17 - 7PH TH 1050 | TITANIUM Tib AL-4V |
|-----------------|---------------------|------------------------------|-----------------------|
| LOX | 0.409 | 0.150 | 0.258 |
| LH ₂ | 0.0254 | 0.00927 | 0.0160 |

CHARACTERISTIC VELOCITY PARAMETER,

$$\sigma \equiv \left(\frac{c}{c_s} \right)^2 (1 - v^2)$$

| FLUID \ DUCT | ALUMINUM 7075-Tb | STEEL 17 - 7 PH TH 1050 | TITANIUM Tib AL-4V |
|-----------------|---------------------|-------------------------------|-----------------------|
| LOX | 0.0595 | 0.0570 | 0.0549 |
| LH ₂ | 0.958 | 0.919 | 0.882 |

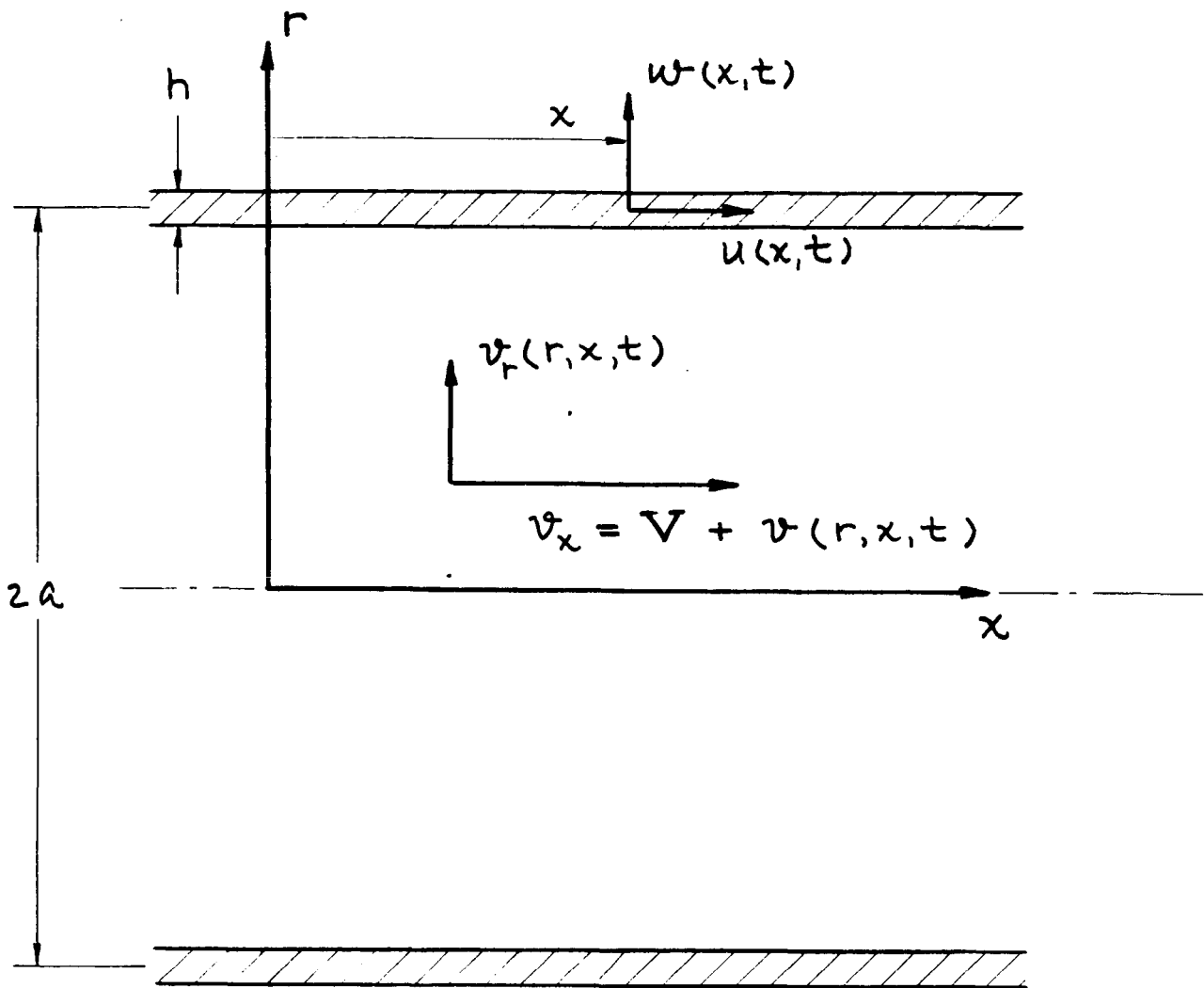
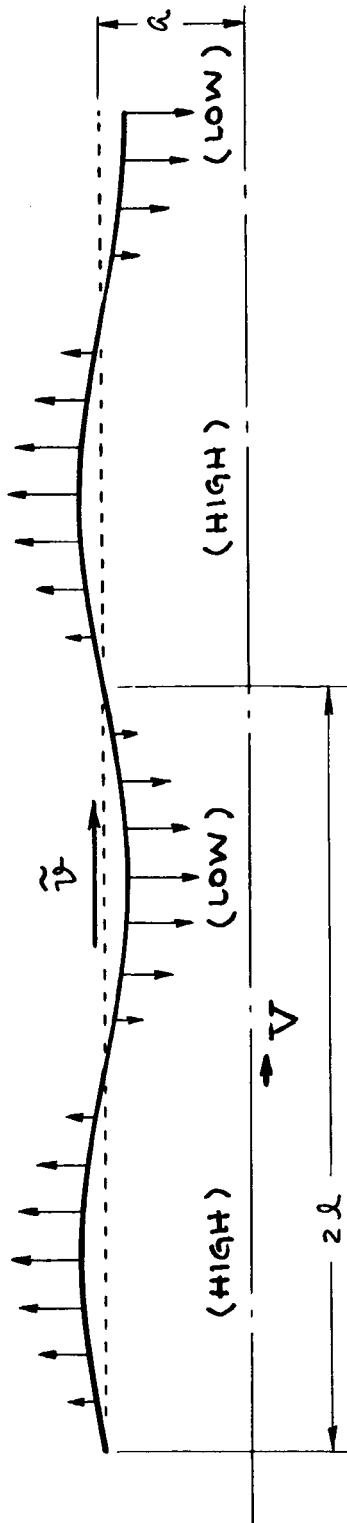


FIGURE 1. COORDINATES, FLUID VELOCITY COMPONENTS & SHELL DISPLACEMENT COMPONENTS

SHELL WALL PRESSURE LOADING FOR $\tilde{v} - V < c$.



SHELL WALL PRESSURE LOADING FOR $\tilde{v} - V > c$.

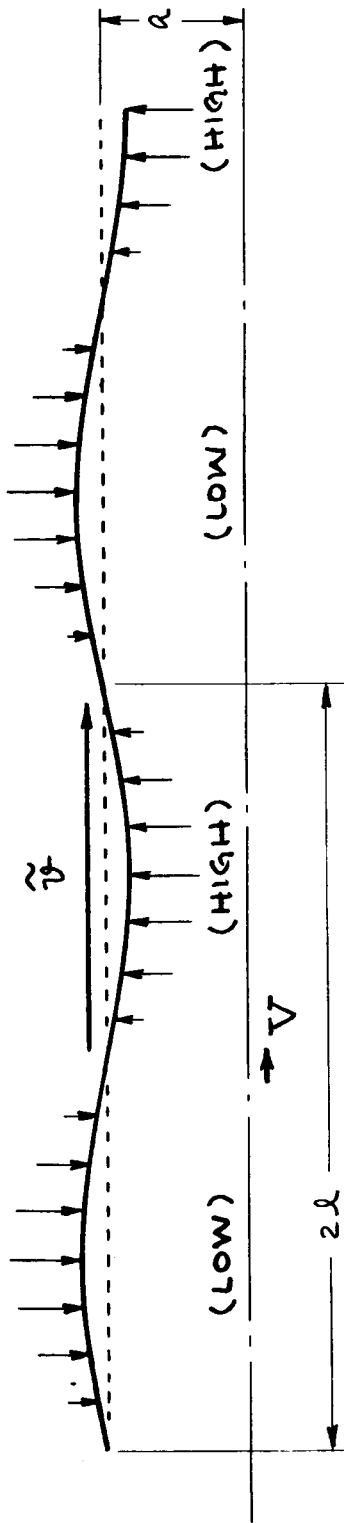


FIGURE 2. TYPICAL SHELL WALL LOADS FOR SUBSONIC & SUPERSONIC PHASE VELOCITIES.

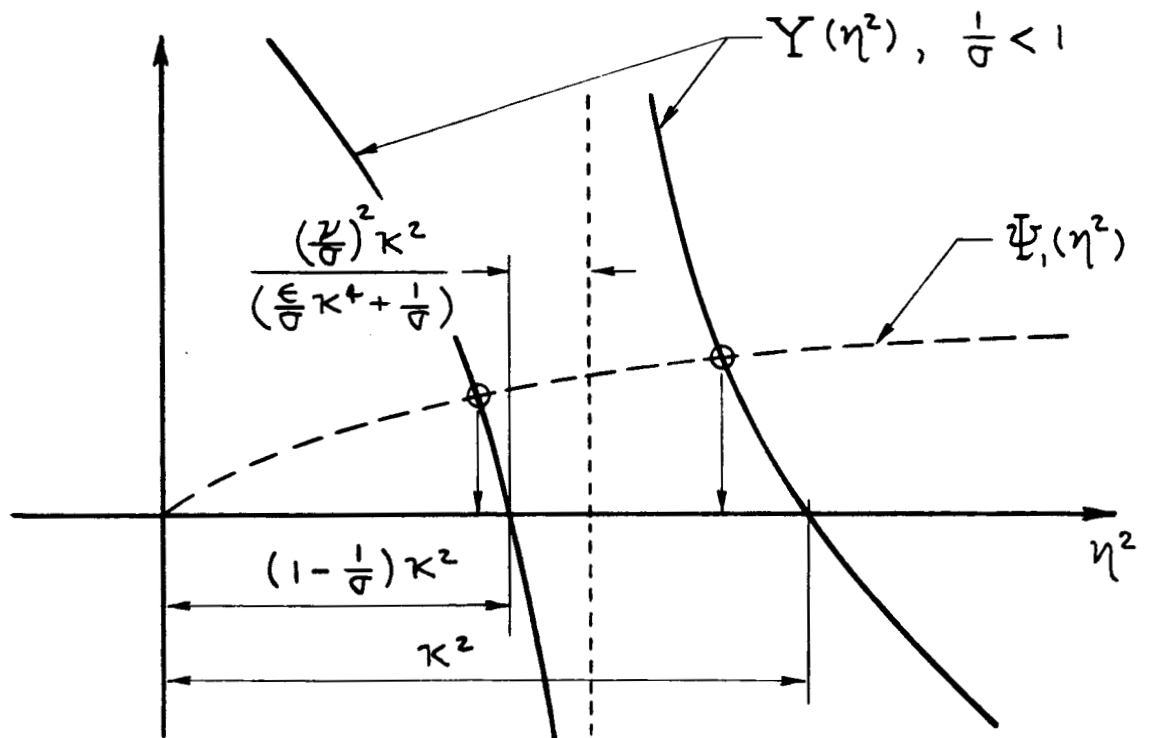
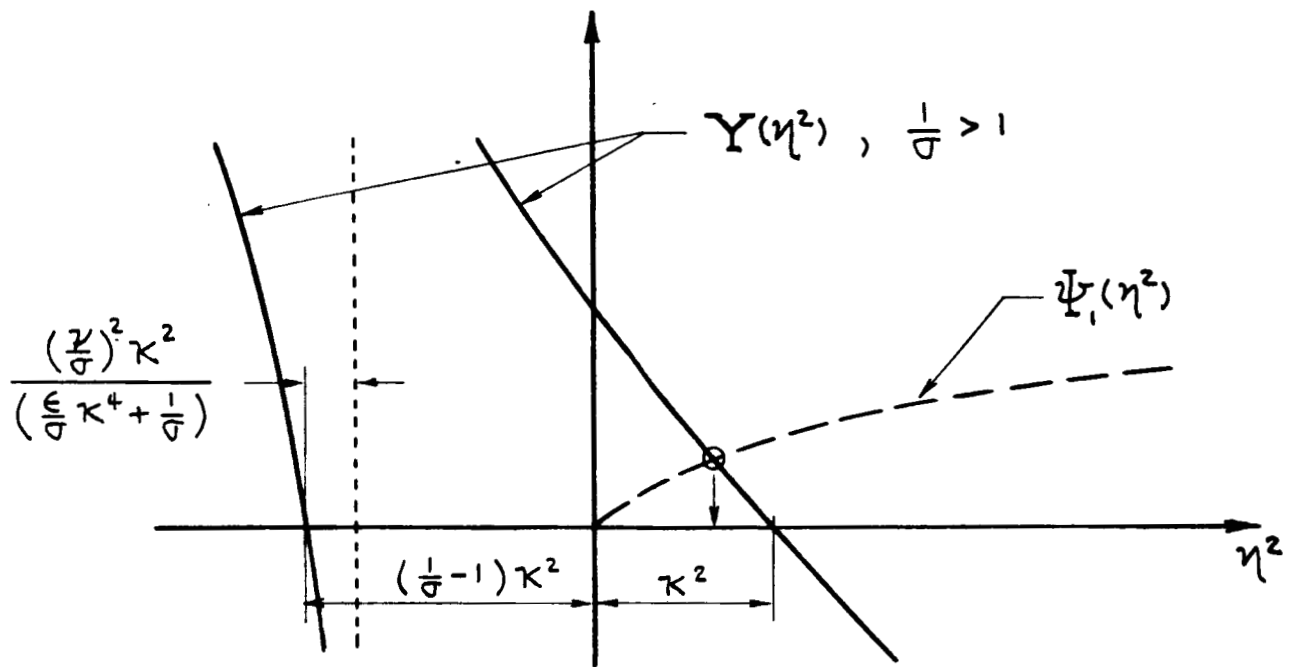


FIGURE 3. THE SIMULTANEOUS SOLUTION, $\psi_1(\eta^2) = Y(\eta^2)$

$$\frac{\psi_2}{\zeta^2 \sigma} = \frac{1}{\zeta^2 \sigma} \cdot \frac{1}{1 - \frac{\mu J_0(\zeta)}{\zeta J_1(\zeta)}}$$

FIGURE 4.

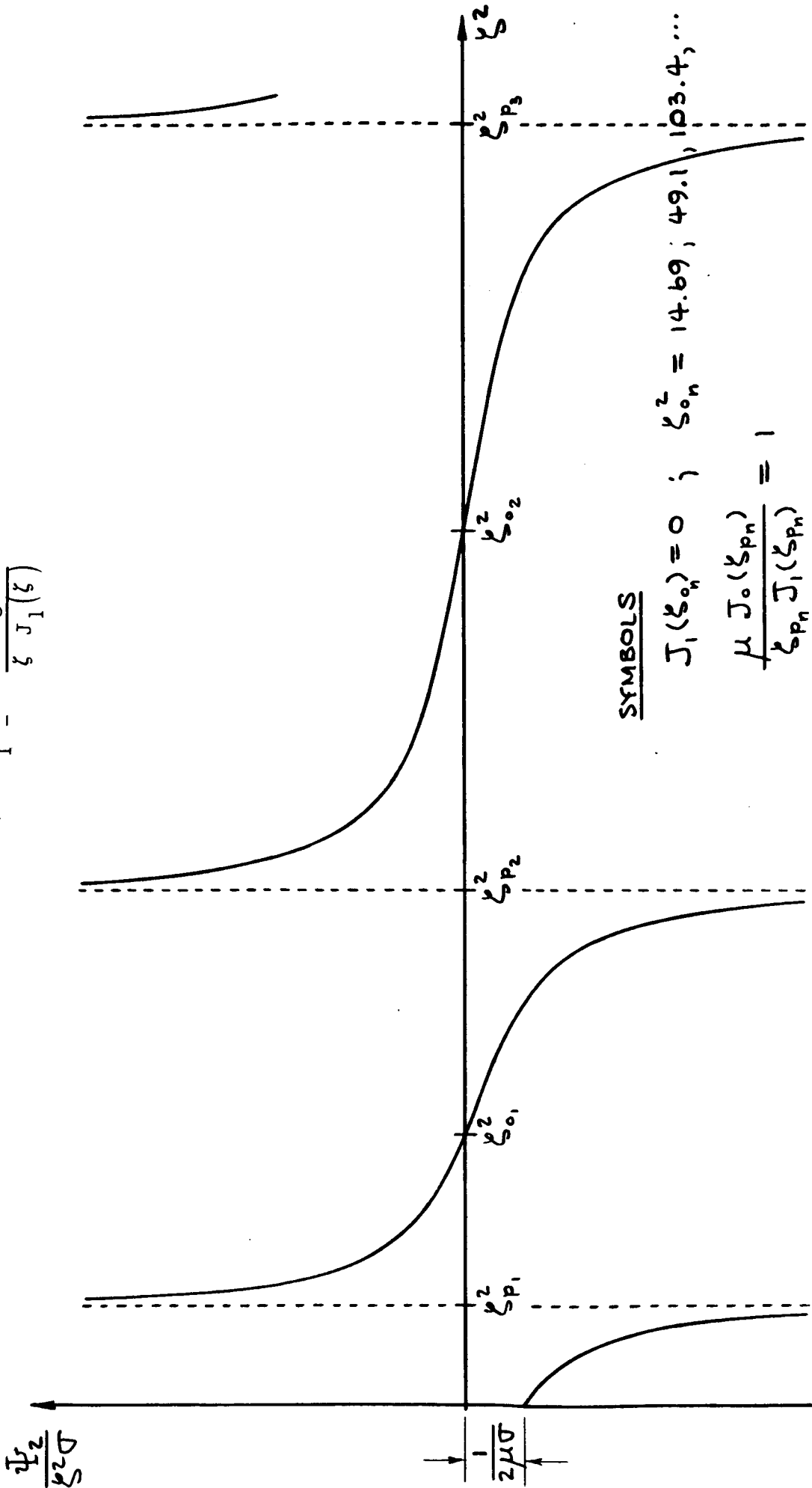


FIGURE 5. $G\left(\frac{\kappa^2}{\zeta^2}\right)$

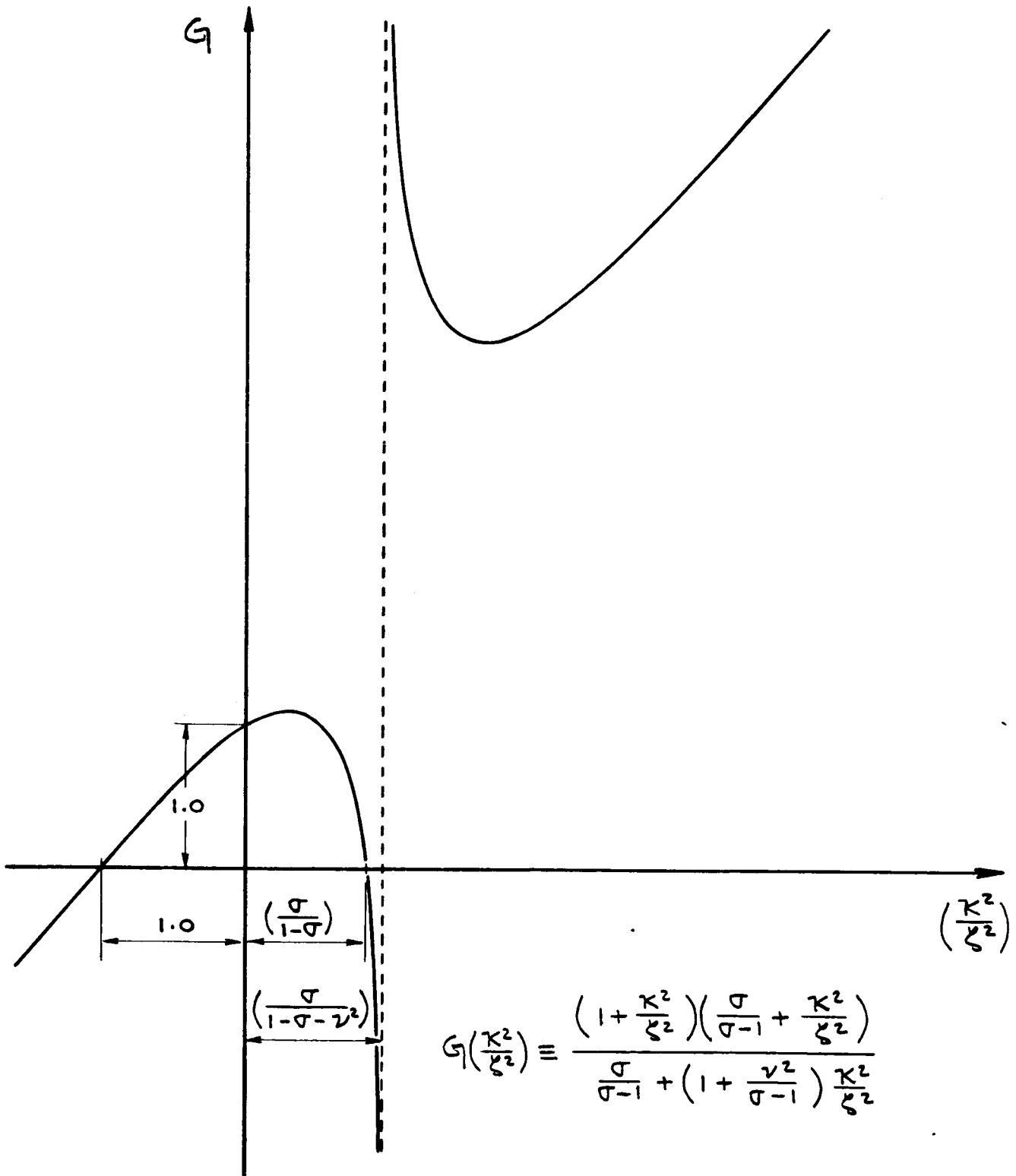
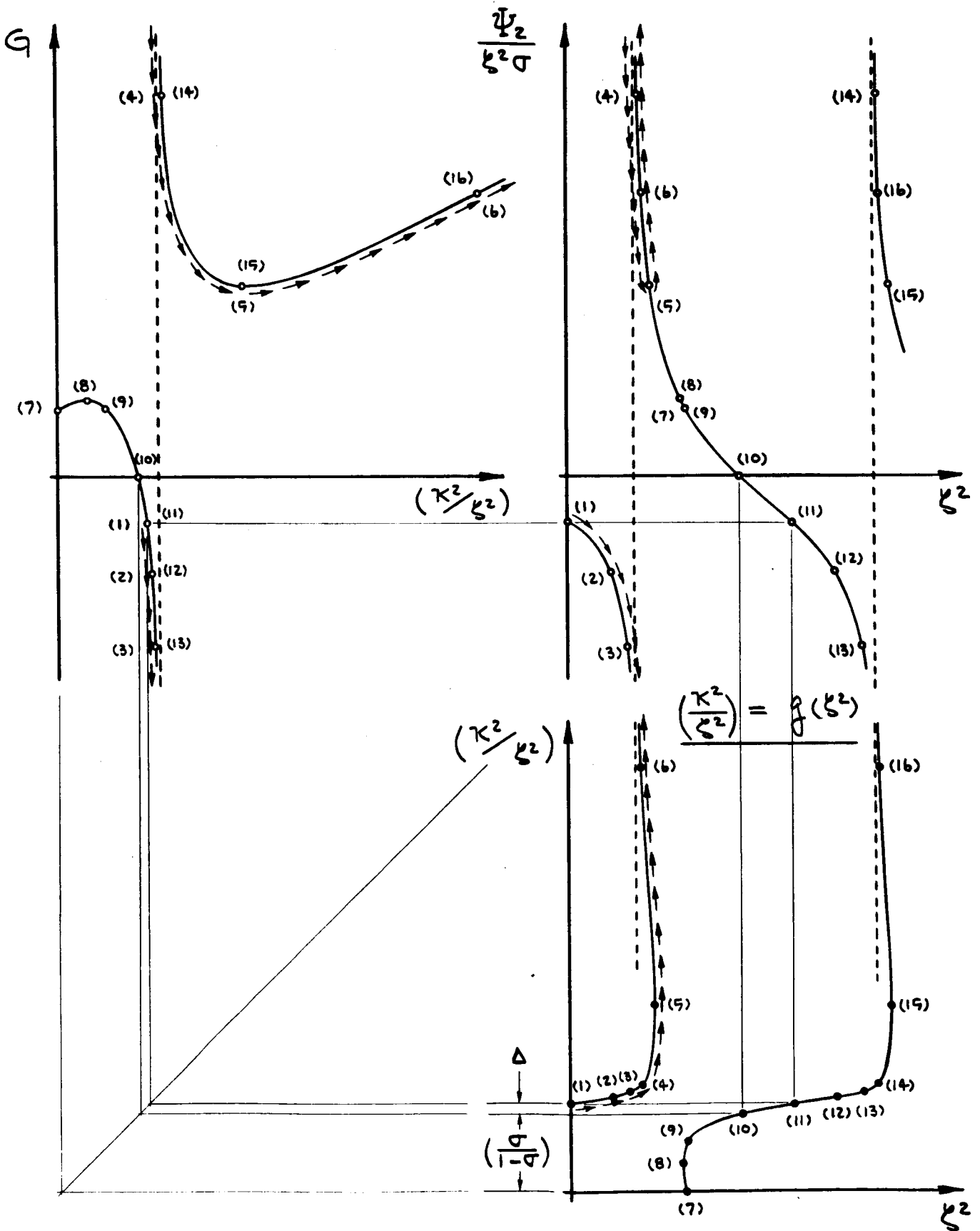


FIGURE 6. MAPPING THE SOLUTION OF $\frac{\psi^2}{\zeta^2 \sigma} = G$



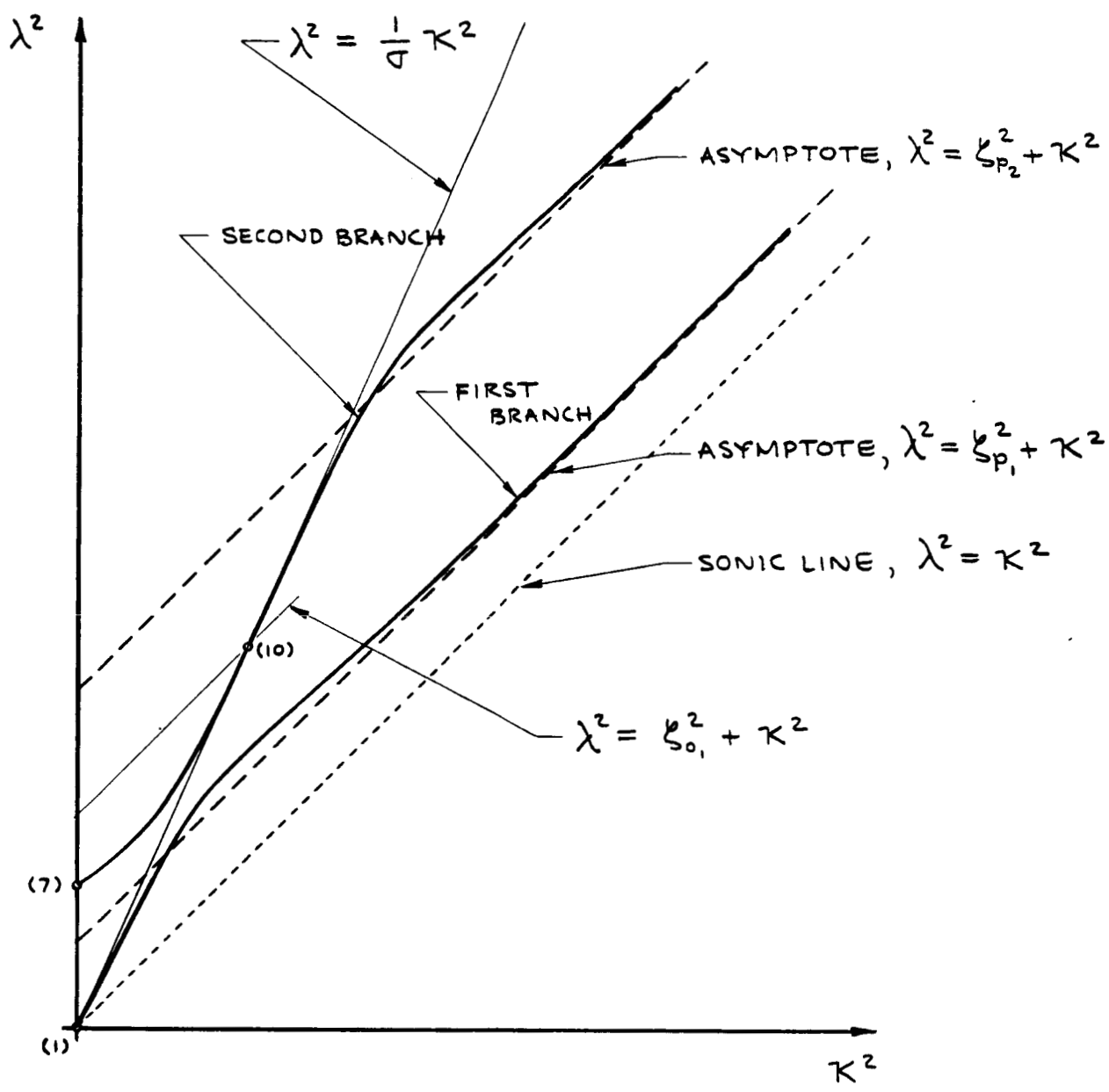
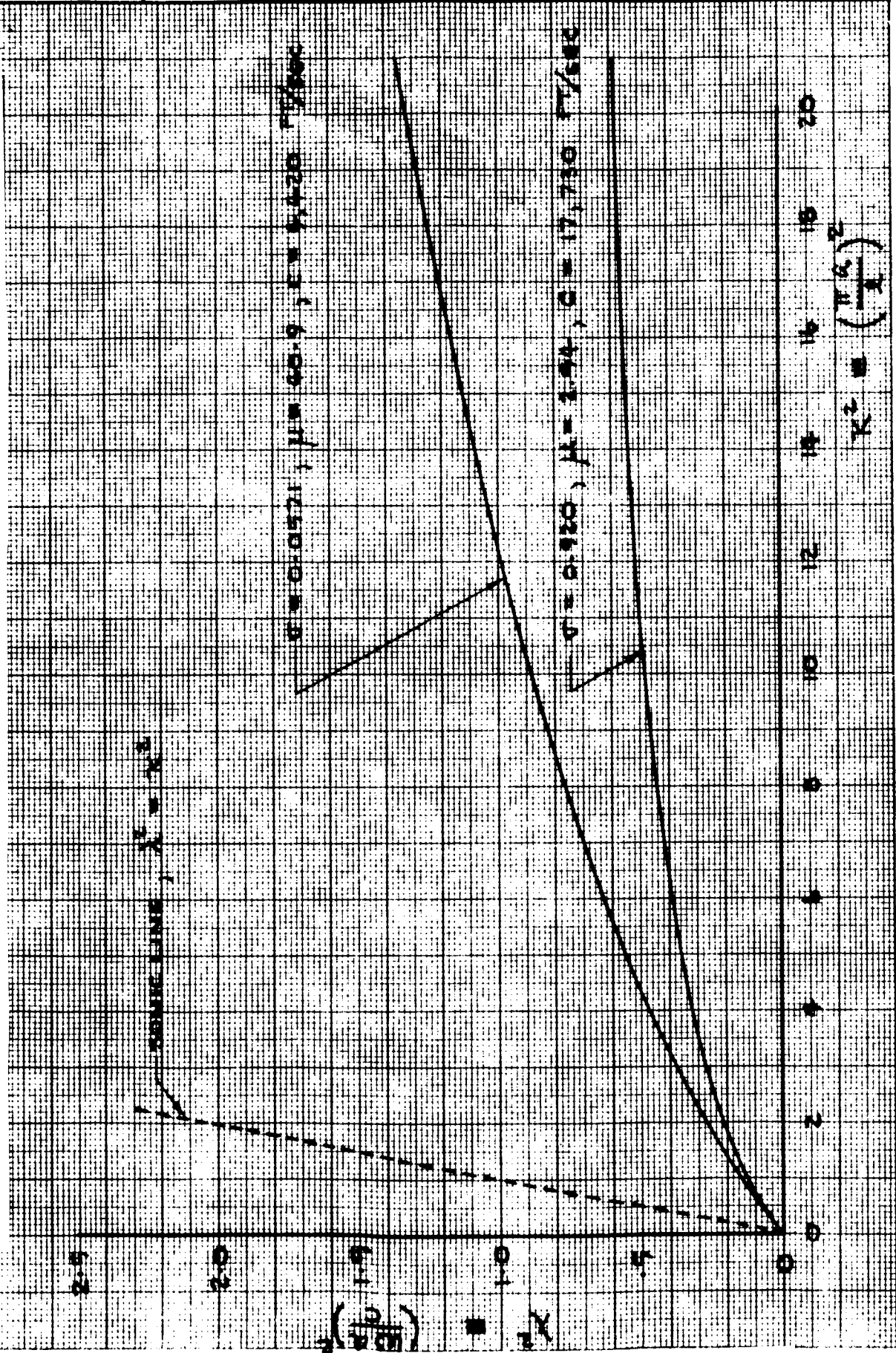


FIGURE 7. SUPERSONIC BRANCHES OF THE FREQUENCY-WAVELENGTH RELATIONSHIP

$$\lambda^2 = \{g(\zeta^2) + 1\} \zeta^2 \quad \text{and} \quad \kappa^2(\zeta^2) \cdot \zeta^2$$

| | | | |
|--------------|---|------------|----|
| PREPARED BY: | NORTH AMERICAN AVIATION, INC. SPACE and INFORMATION SYSTEMS DIVISION | PAGE NO. | OF |
| CHECKED BY: | | REPORT NO. | |
| DATE: | | MODEL NO. | |

FIGURE 8. THE LOWER BRANCH FREQUENCY - WAVELENGTH RELATIONSHIP



PREPARED BY:

NORTH AMERICAN AVIATION, INC.
SPACE and INFORMATION SYSTEMS DIVISION

PAGE NO. OF

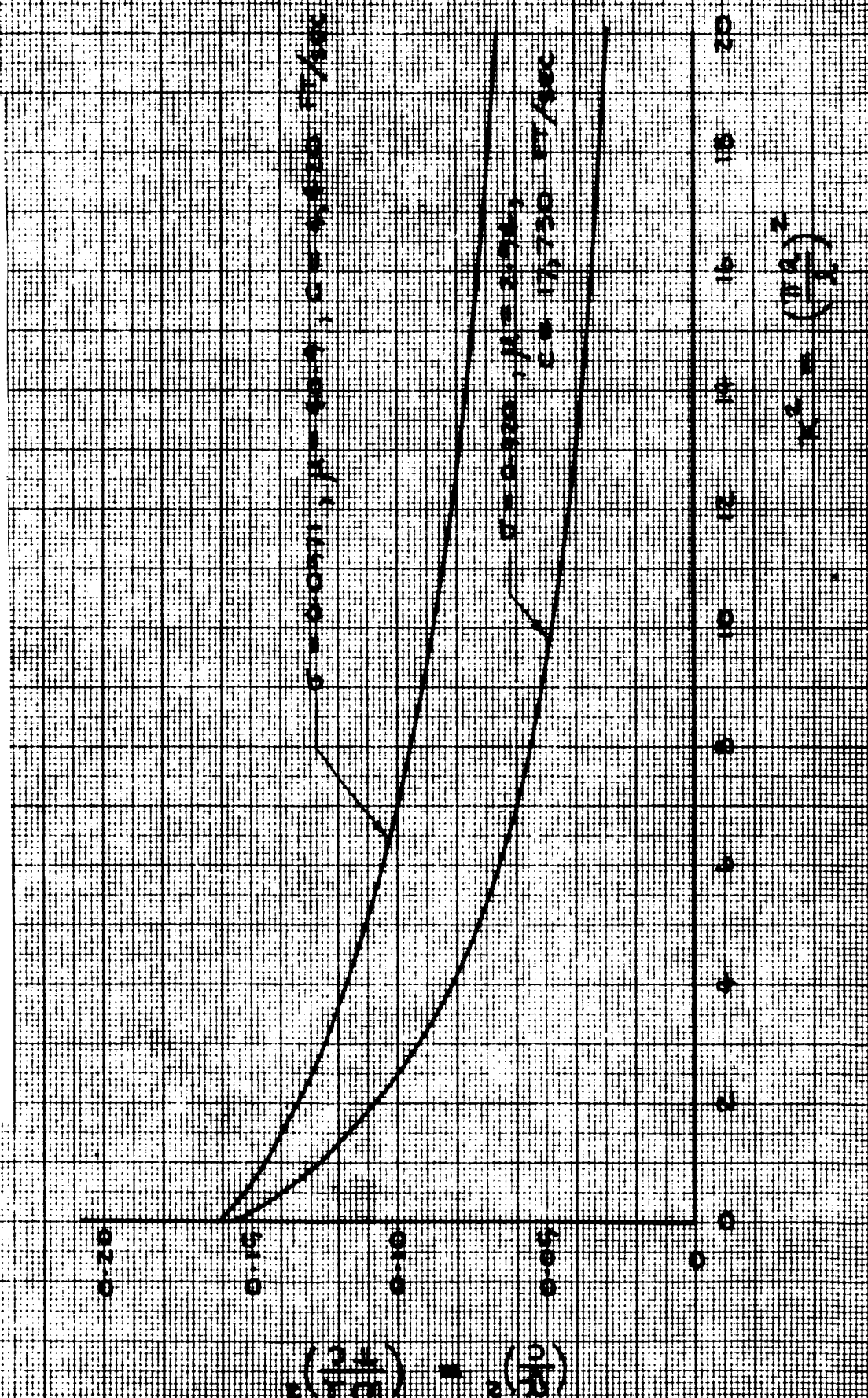
CHECKED BY:

REPORT NO.

DATE:

MODEL NO.

FIGURE 9. THE LOWER BRANCH PHASE VELOCITY VS WAVE NUMBER RELATIONSHIP



PREPARED BY:

NORTH AMERICAN AVIATION, INC.
SPACE and INFORMATION SYSTEMS DIVISION

PAGE NO. OF

CHECKED BY:

REPORT NO.

DATE:

MODEL NO.

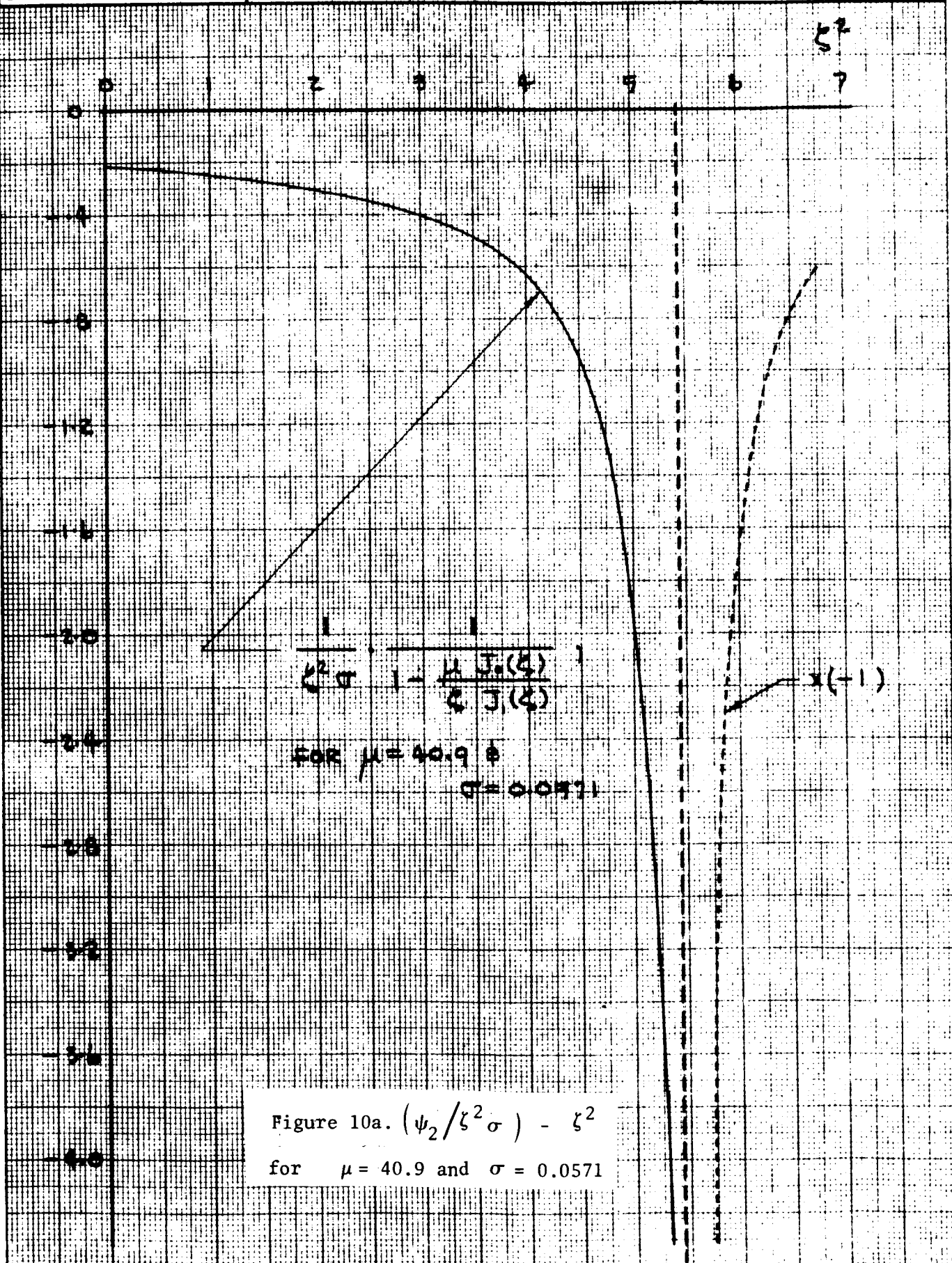
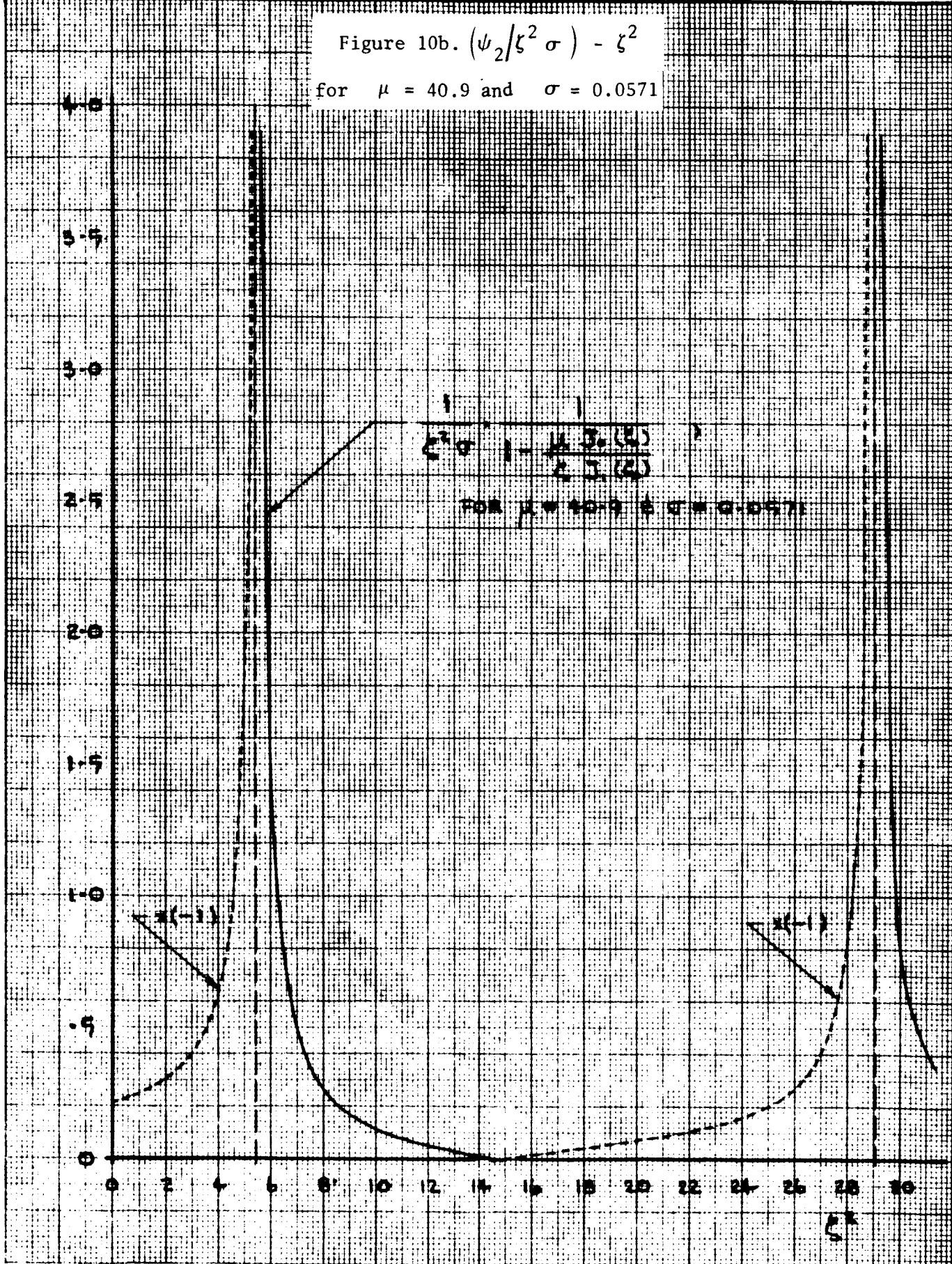


Figure 10a. $(\psi_2 / z^2 \sigma) - z^2$
for $\mu = 40.9$ and $\sigma = 0.0571$

| | | | |
|--------------|---|------------|----|
| PREPARED BY: | NORTH AMERICAN AVIATION, INC. SPACE and INFORMATION SYSTEMS DIVISION | PAGE NO. | OF |
| CHECKED BY: | | REPORT NO. | |
| DATE: | | MODEL NO. | |

Figure 10b. $(\psi_2 / \zeta^2 \sigma) - \zeta^2$
for $\mu = 40.9$ and $\sigma = 0.0571$



PREPARED BY:

NORTH AMERICAN AVIATION, INC.
SPACE and INFORMATION SYSTEMS DIVISION

PAGE NO. OF

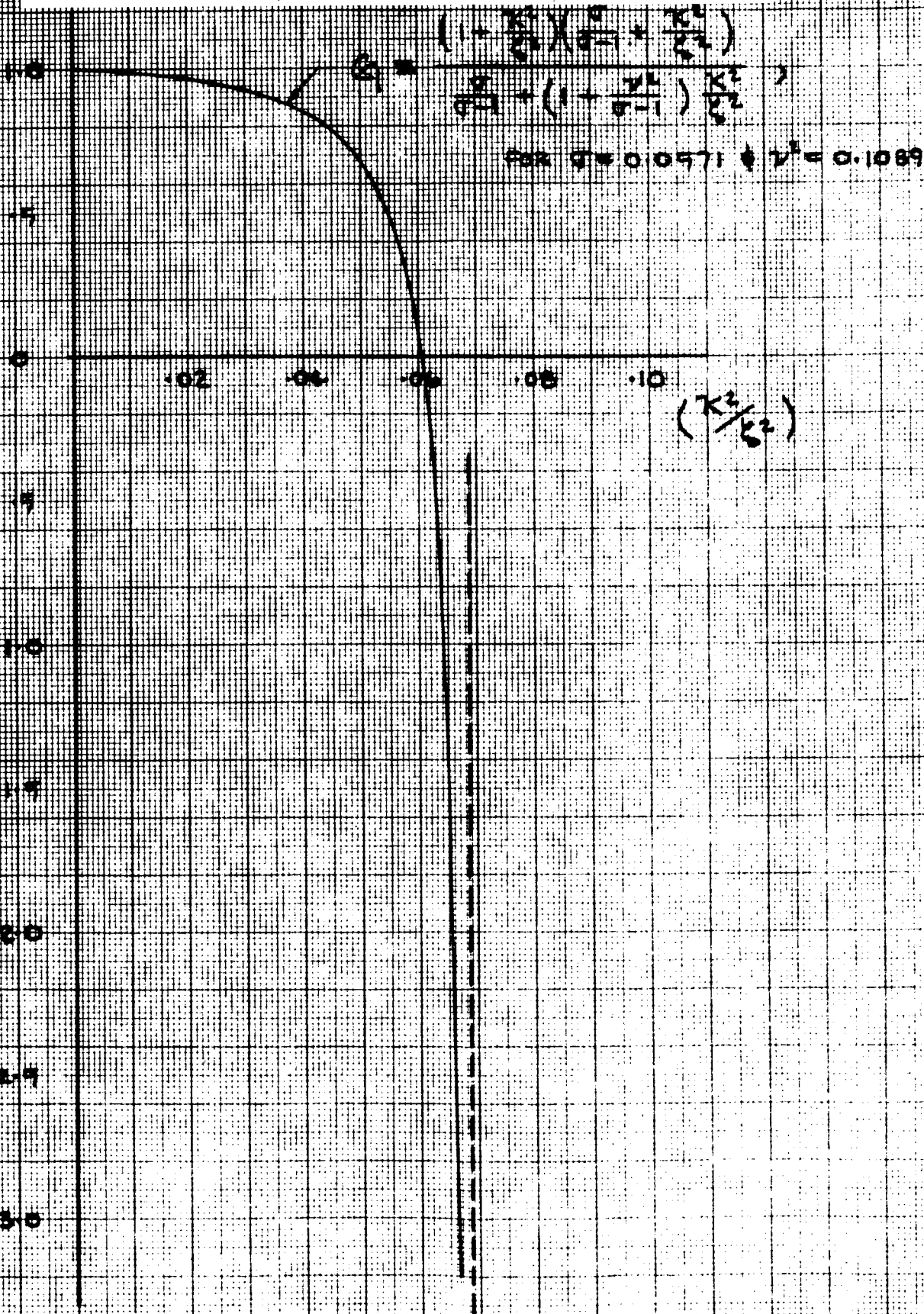
CHECKED BY:

REPORT NO.

DATE:

MODEL NO.

Figure 11a. $G - (\kappa^2/\zeta^2)$ for $\sigma = 0.0571$ and $\nu^2 = 0.1089$



PREPARED BY:

NORTH AMERICAN AVIATION, INC.
SPACE and INFORMATION SYSTEMS DIVISION

PAGE NO. OF

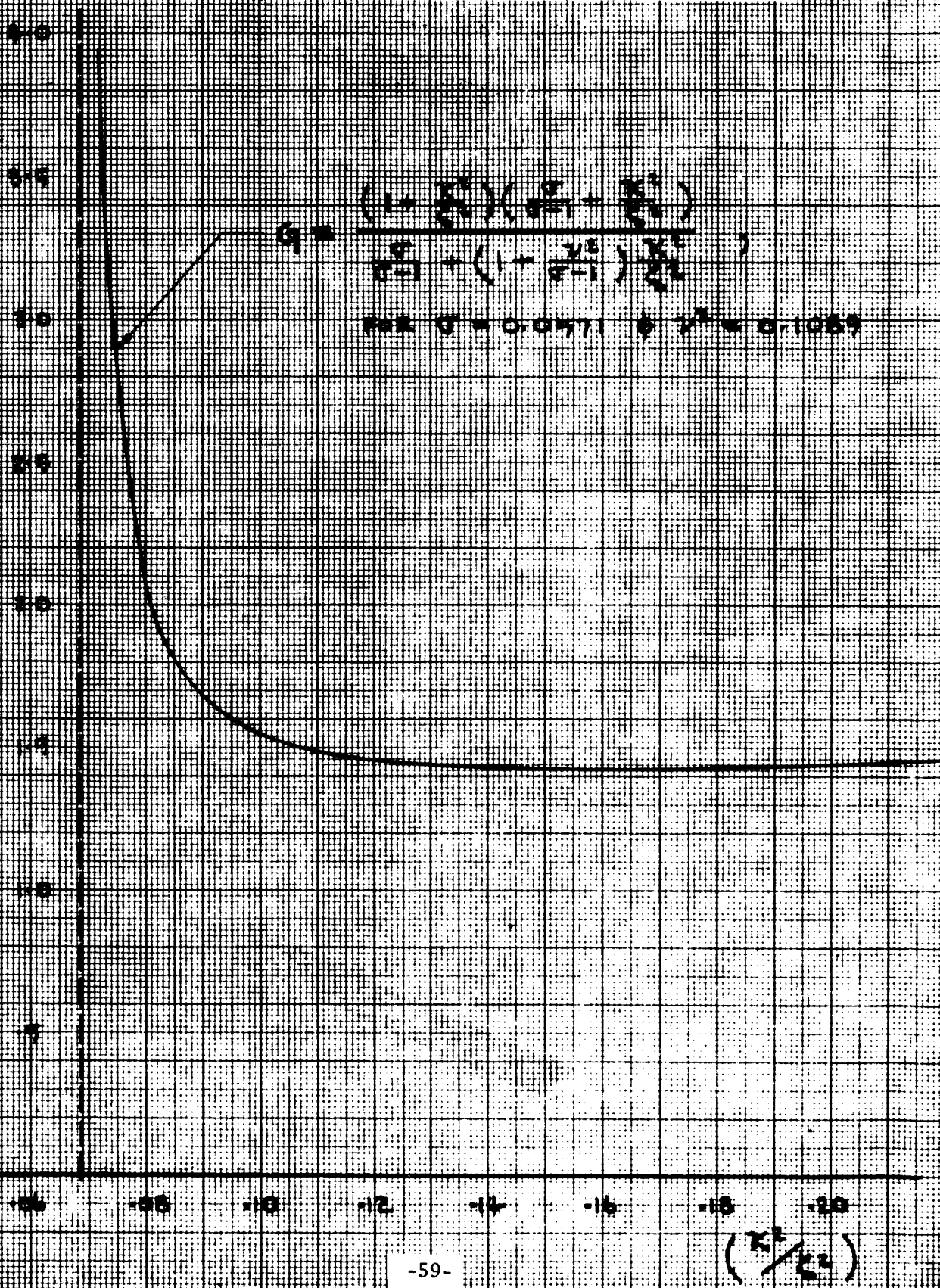
CHECKED BY:

REPORT NO.

DATE:

MODEL NO.

Figure 11b. $G - (\kappa^2/\zeta^2)$ for $\sigma = 0.0571$ and $\nu^2 = 0.1089$



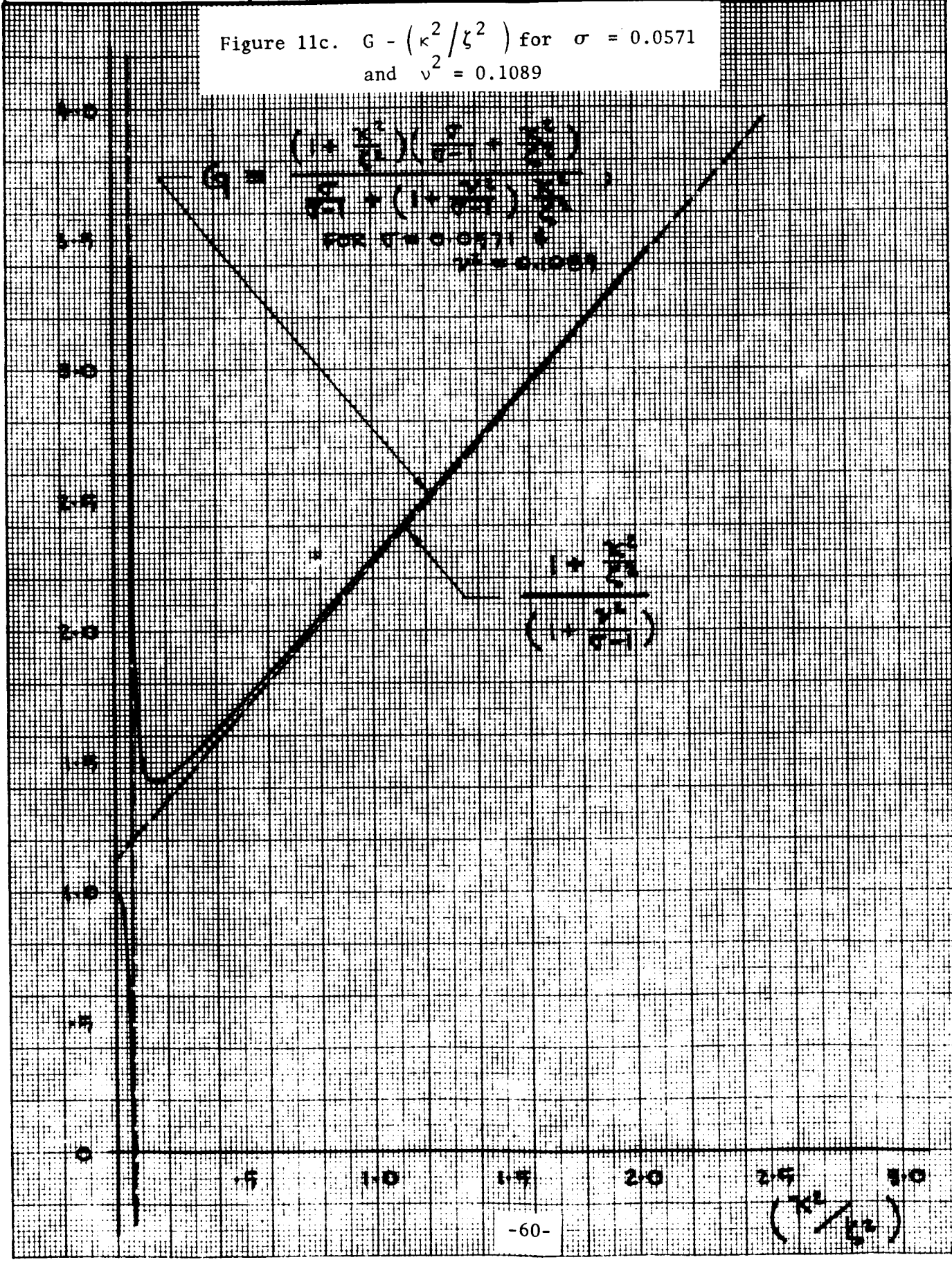
$\left(\frac{\kappa^2}{\zeta^2}\right)$

PREPARED BY:
 CHECKED BY:
 DATE:

NORTH AMERICAN AVIATION, INC.
 SPACE and INFORMATION SYSTEMS DIVISION

PAGE NO. OF
 REPORT NO.
 MODEL NO.

Figure 11c. $G - (\kappa^2 / \zeta^2)$ for $\sigma = 0.0571$
 and $\nu^2 = 0.1089$



PREPARED BY:

NORTH AMERICAN AVIATION, INC.
SPACE and INFORMATION SYSTEMS DIVISION

PAGE NO. OF

CHECKED BY:

REPORT NO.

DATE:

MODEL NO.

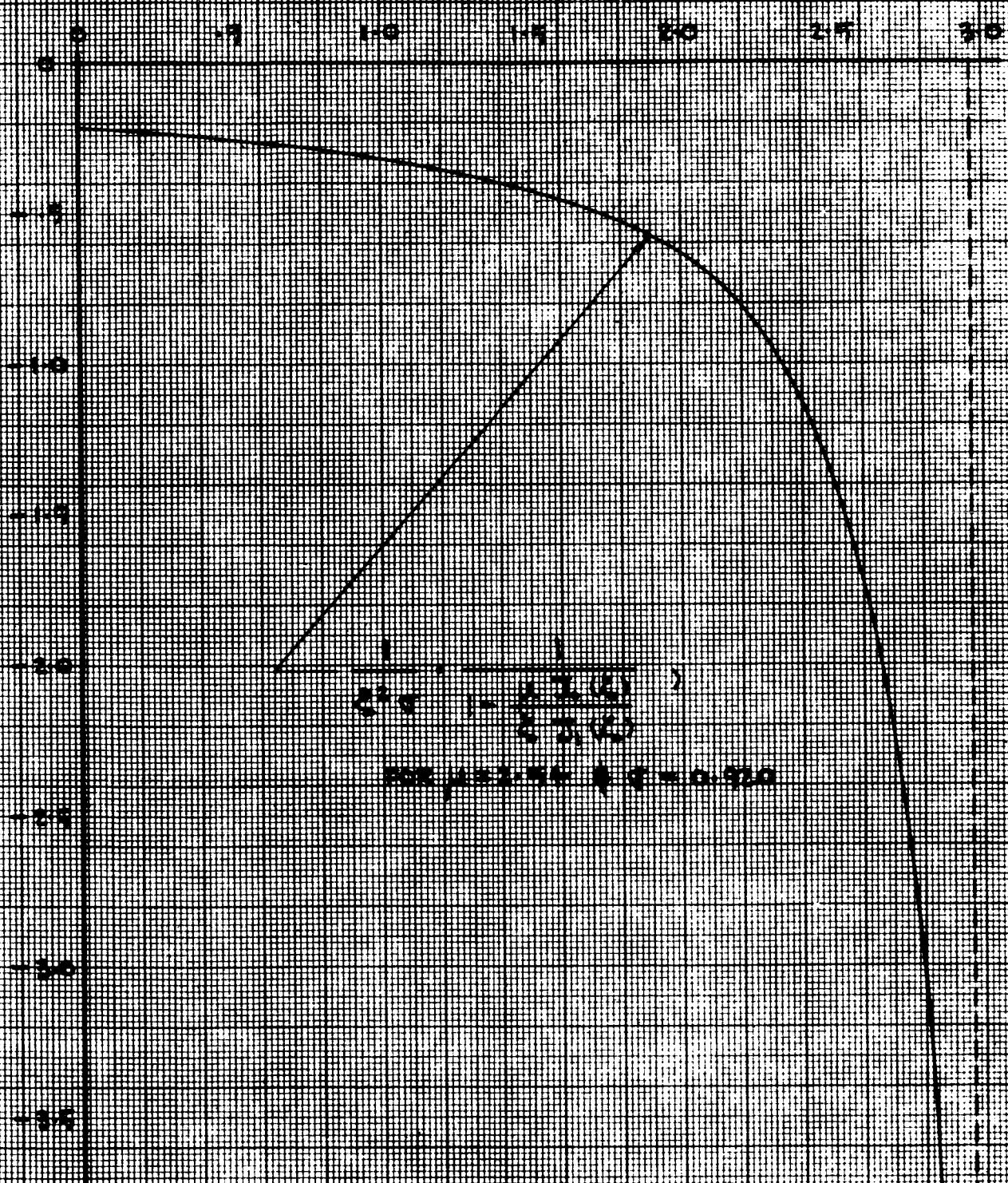
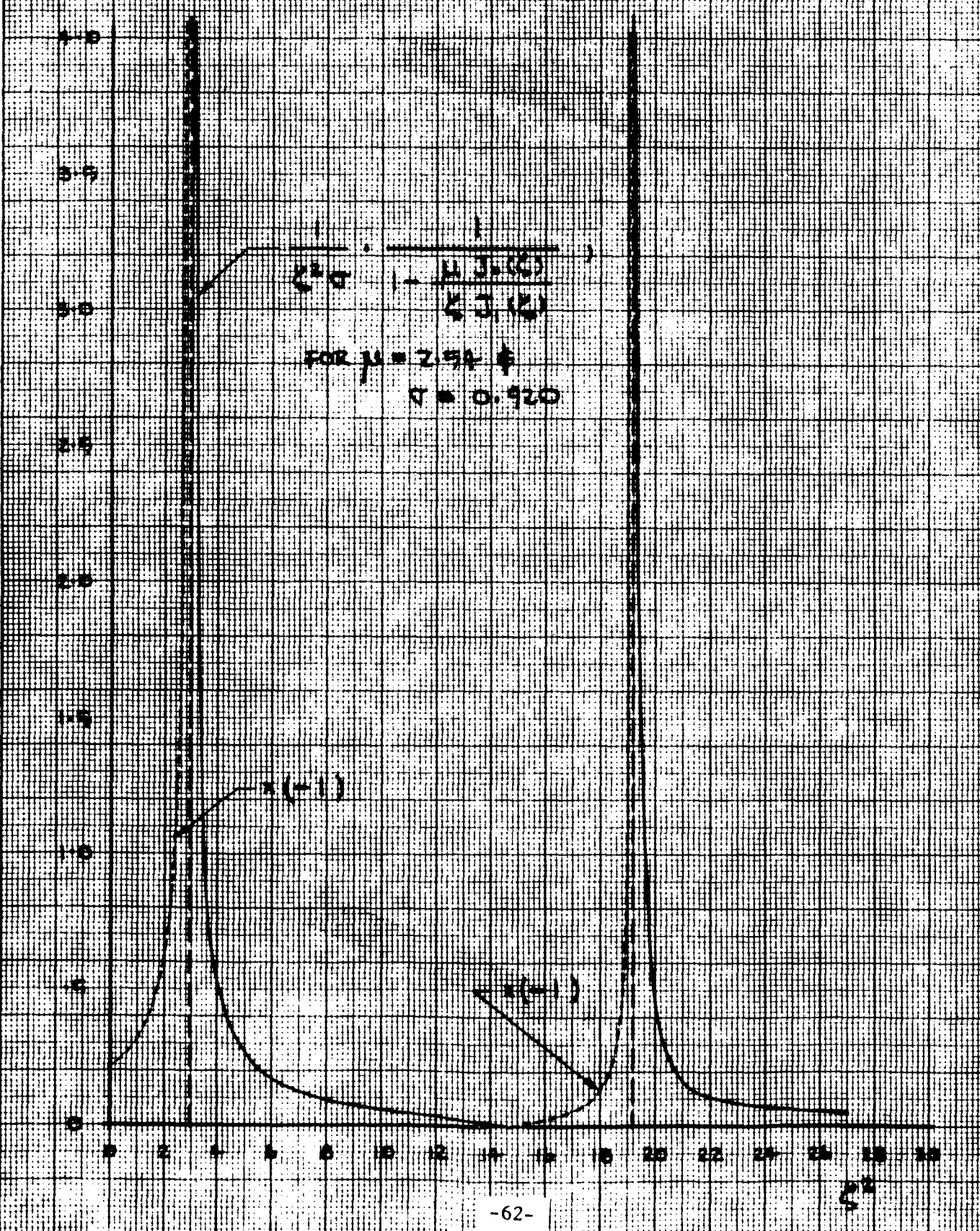


Figure 12a. $\left(\frac{\psi_2}{\zeta^2 \sigma}\right) - \zeta^2$ for $\mu = 2.54$ and $\sigma = 0.920$

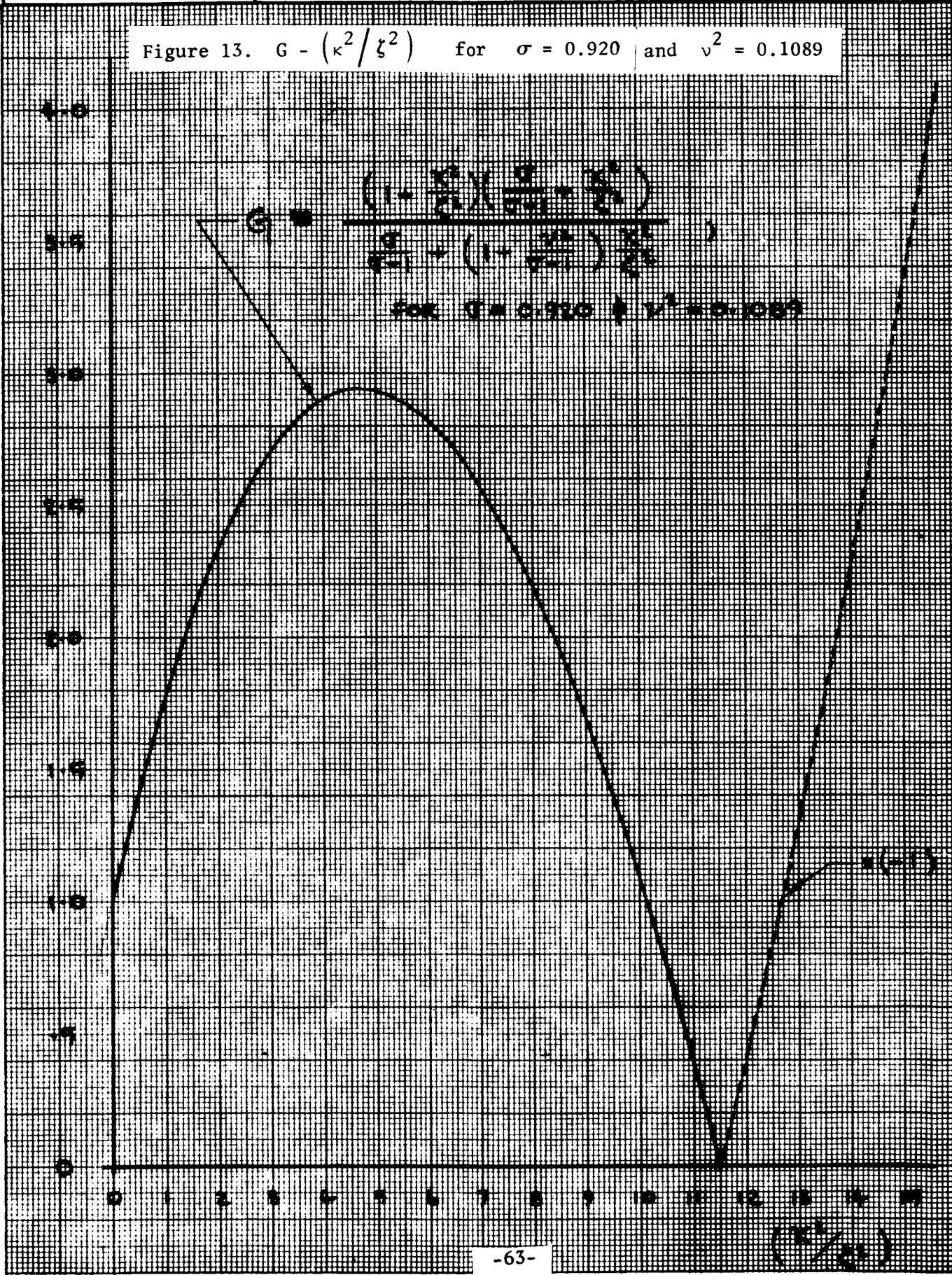
| | | | |
|--------------|---|------------|----|
| PREPARED BY: | NORTH AMERICAN AVIATION, INC. SPACE and INFORMATION SYSTEMS DIVISION | PAGE NO. | OF |
| CHECKED BY: | | REPORT NO. | |
| DATE: | | MODEL NO. | |

Figure 12b. $(\psi_2 / \zeta^2 \sigma) - \zeta^2$ for $\mu = 2.54$ and $\sigma = 0.920$

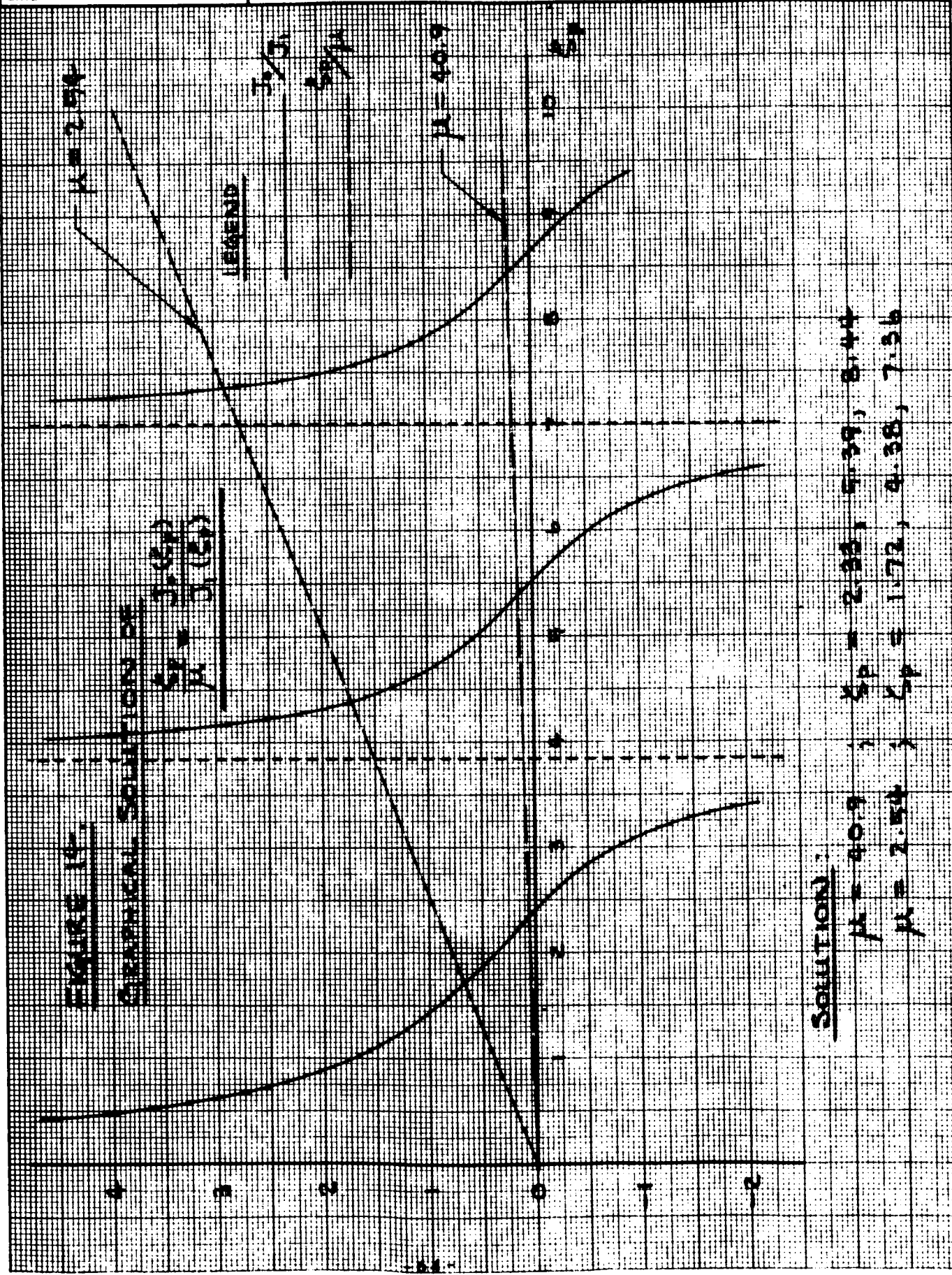


| | | | |
|--------------|---|------------|----|
| PREPARED BY: | NORTH AMERICAN AVIATION, INC. SPACE and INFORMATION SYSTEMS DIVISION | PAGE NO. | OF |
| CHECKED BY: | | REPORT NO. | |
| DATE: | | MODEL NO. | |

Figure 13. $G - (\kappa^2 / \zeta^2)$ for $\sigma = 0.920$ and $v^2 = 0.1089$

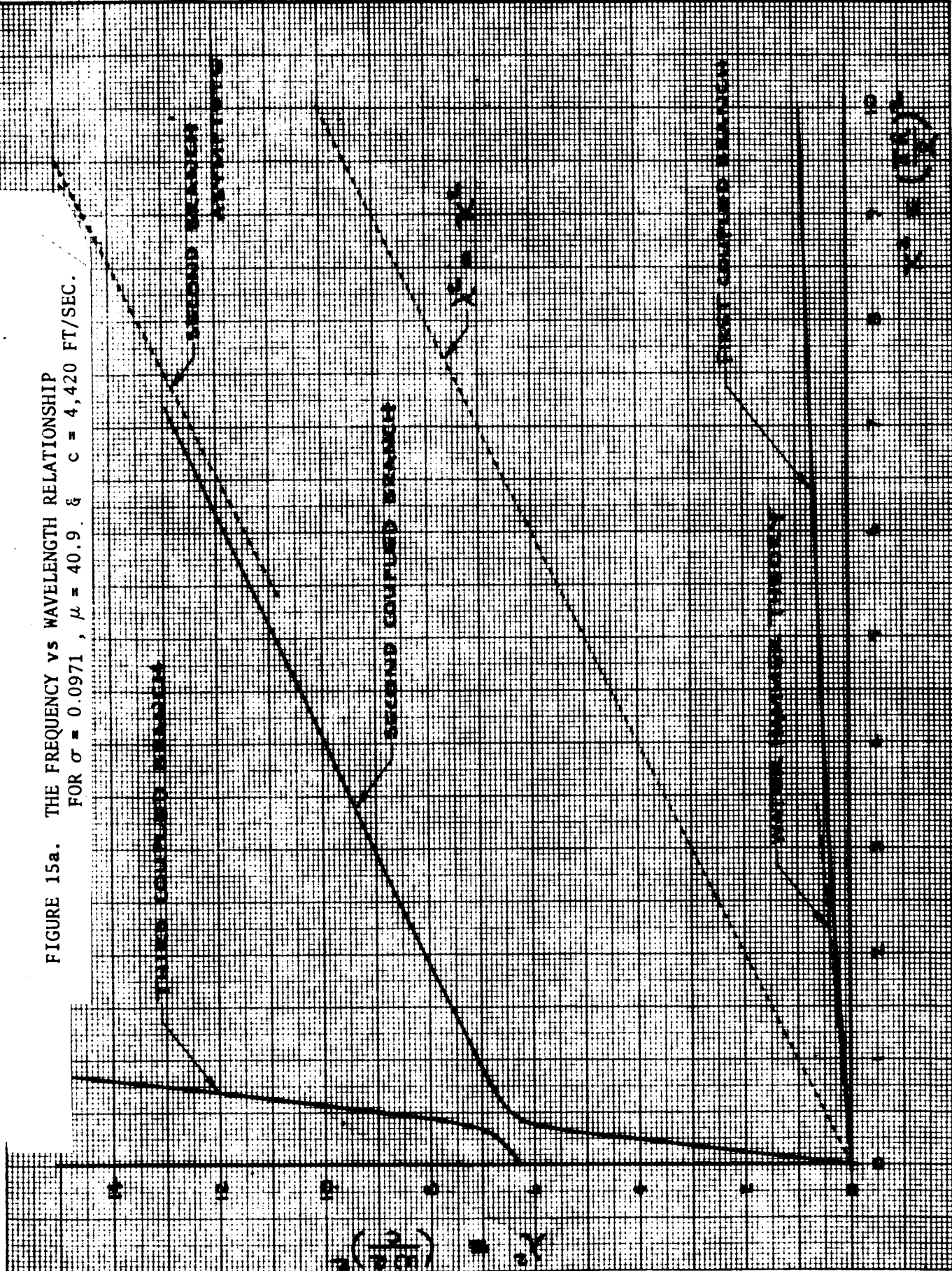


| | | | |
|--------------|--|------------|----|
| PREPARED BY: | NORTH AMERICAN AVIATION, INC. SPACE and INFORMATION SYSTEMS DIVISION | PAGE NO. | OF |
| CHECKED BY: | | REPORT NO. | |
| DATE: | | MODEL NO. | |



| | | | |
|--------------|---|------------|----|
| PREPARED BY: | NORTH AMERICAN AVIATION, INC. SPACE and INFORMATION SYSTEMS DIVISION | PAGE NO. | OF |
| CHECKED BY: | | REPORT NO. | |
| DATE: | | MODEL NO. | |

FIGURE 15a. THE FREQUENCY vs WAVELENGTH RELATIONSHIP
FOR $\sigma = 0.0971$, $\mu = 40.9$ & $c = 4,420$ FT/SEC.



PREPARED BY:

NORTH AMERICAN AVIATION, INC.
SPACE and INFORMATION SYSTEMS DIVISION

PAGE NO. OF

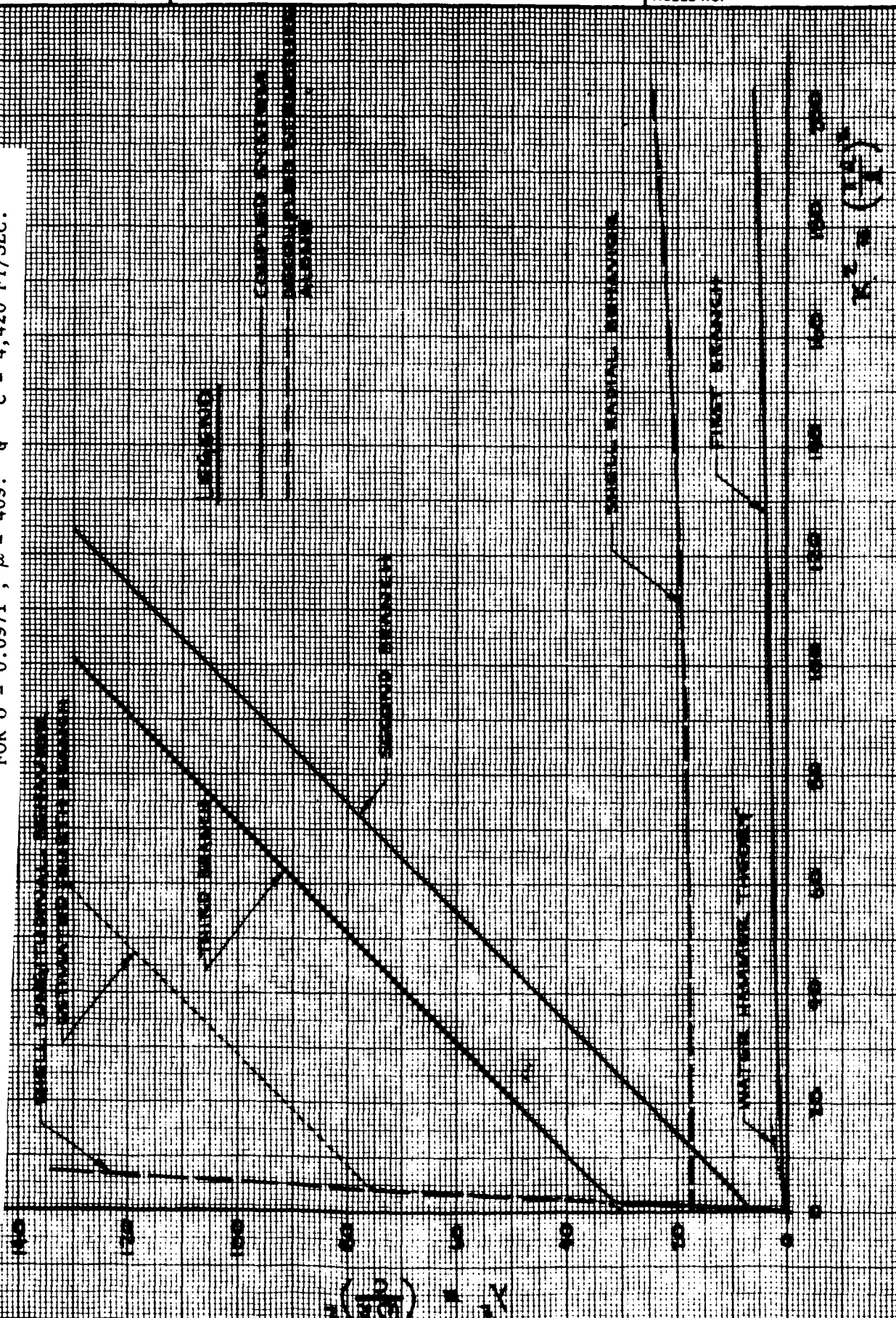
CHECKED BY:

REPORT NO.

DATE:

MODEL NO.

FIGURE 15b. THE FREQUENCY vs WAVELENGTH RELATIONSHIP
FOR $\sigma = 0.0971$, $\mu = 409$. & $c = 4,420$ FT/SEC.



PREPARED BY:

NORTH AMERICAN AVIATION, INC.
SPACE and INFORMATION SYSTEMS DIVISION

PAGE NO. OF

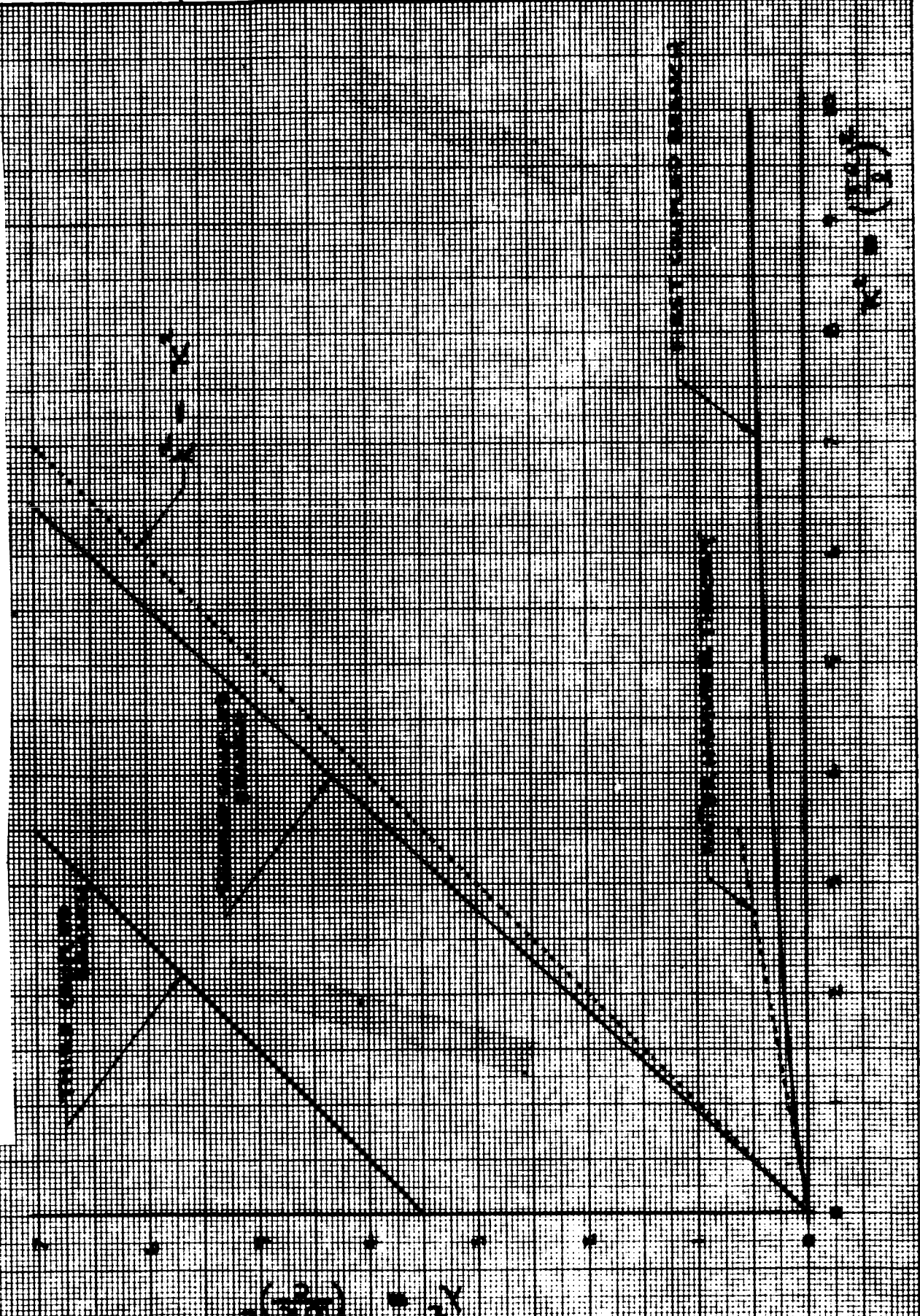
CHECKED BY:

REPORT NO.

DATE:

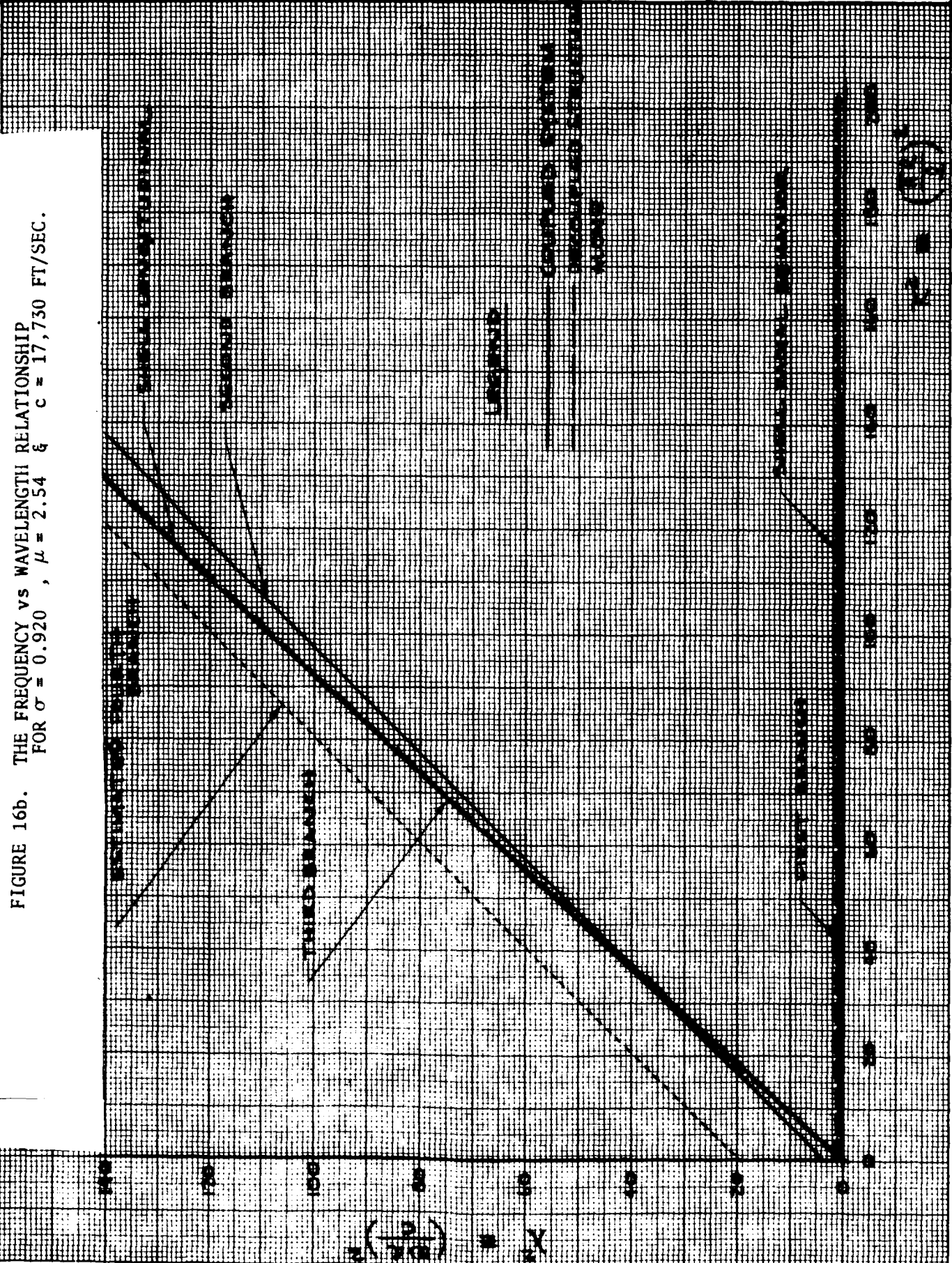
MODEL NO.

FIGURE 16a, THE FREQUENCY vs WAVELENGTH RELATIONSHIP
 FOR $\mu = 0.920$, $\mu = 2.54$ & $c = 17,730$ FT/SEC.



| | | | |
|--------------|---|------------|----|
| PREPARED BY: | NORTH AMERICAN AVIATION, INC. SPACE and INFORMATION SYSTEMS DIVISION | PAGE NO. | OF |
| CHECKED BY: | | REPORT NO. | |
| DATE: | | MODEL NO. | |

FIGURE 16b. THE FREQUENCY vs WAVELENGTH RELATIONSHIP
FOR $\sigma = 0.920$, $\mu = 2.54$ & $c = 17,730$ FT/SEC.



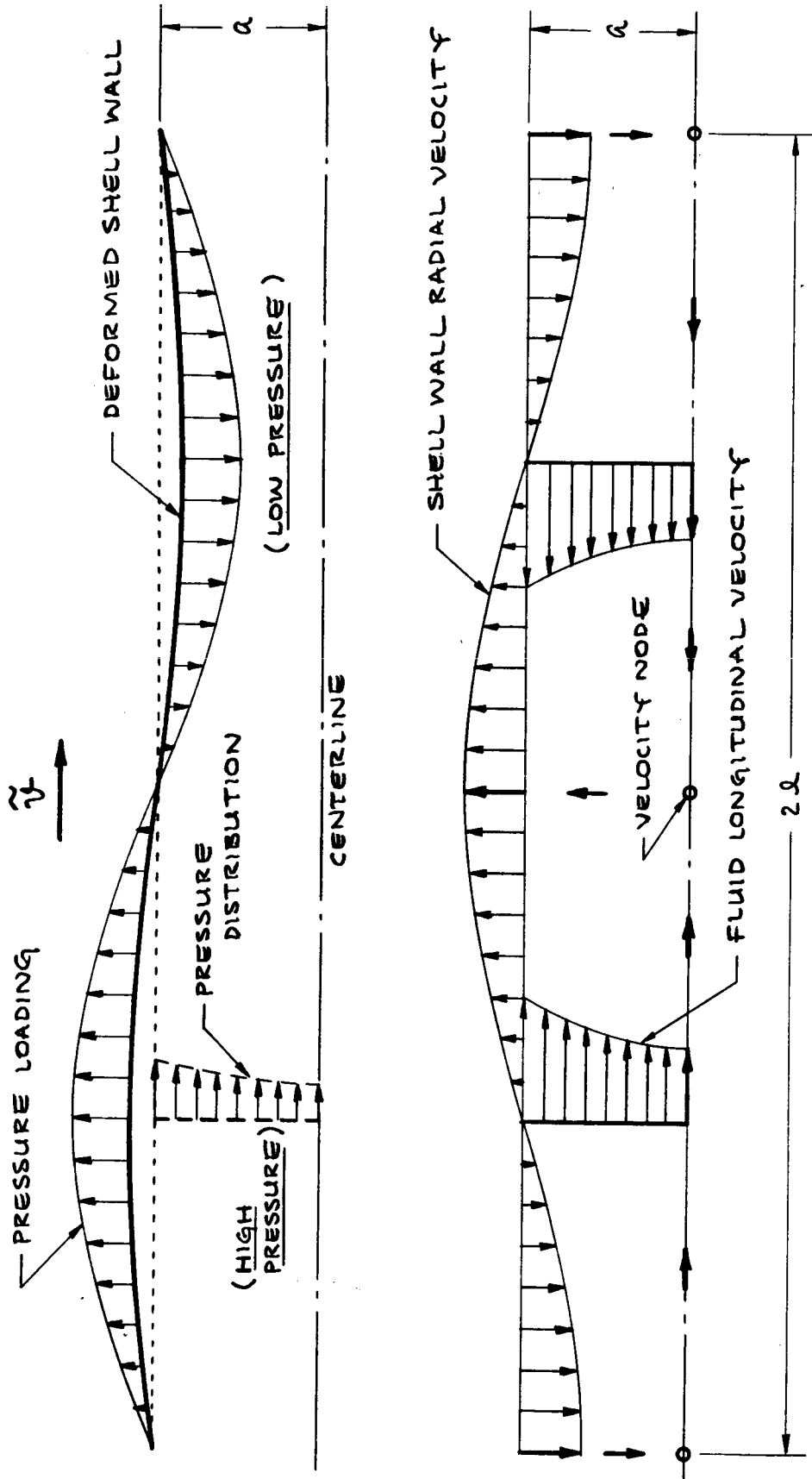


FIGURE 17a. RESPONSE TYPICAL OF THE HYDROELASTIC PROPAGATING WAVE HAVING THE SUBSONIC PHASE VELOCITY.

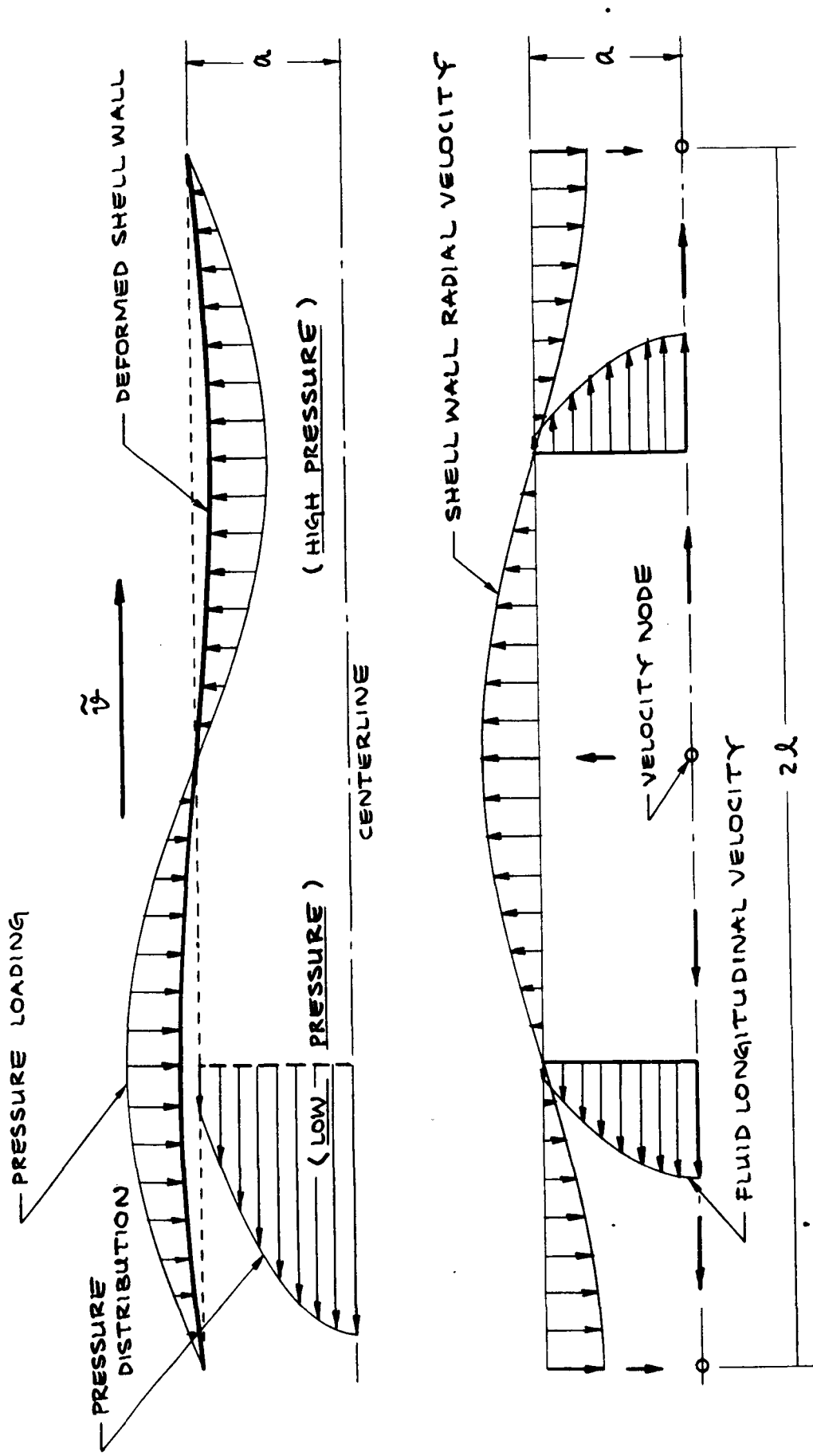


FIGURE 17 b. RESPONSE TYPICAL OF THE HYDROELASTIC PROPAGATING WAVE HAVING THE SUPERSONIC FIRST MODE PHASE VELOCITY

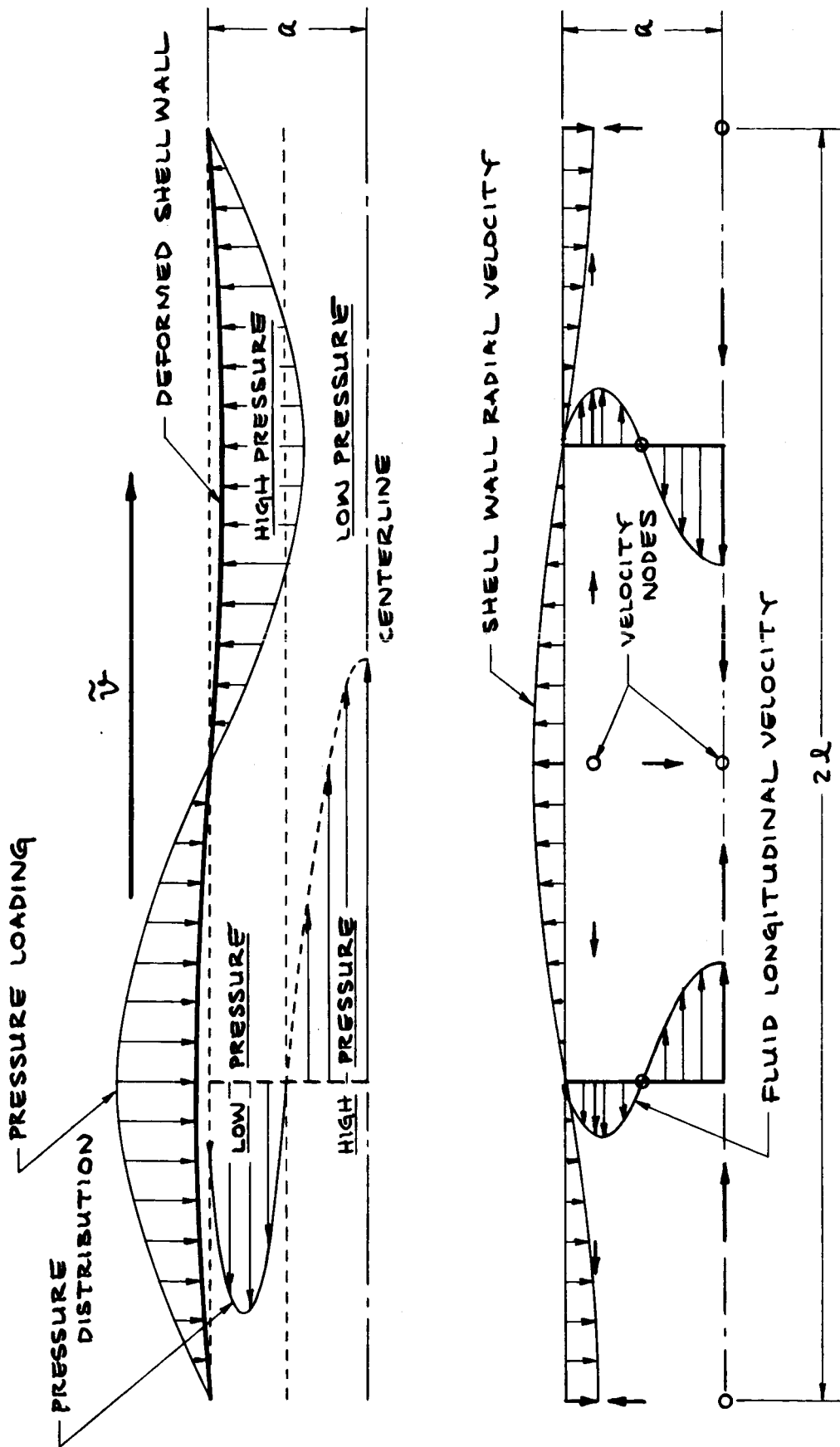


FIGURE 17c. RESPONSE TYPICAL OF THE HYDROELASTIC PROPAGATING WAVE HAVING THE SUPERSONIC SECOND MODE PHASE VELOCITY